Impact of physico-chemical properties of nanocellulose on rheology of aqueous suspensions and its utility in multiple fields: A review

Rana, Ashvinder Kumar; Thakur, Vijay Kumar

Published in:
Journal of Vinyl and Additive Technology

DOI:
10.1002/vnl.22006

First published: 18/04/2023

Document Version
Publisher's PDF, also known as Version of record

Received: 31 December 2022 | Revised: 2 April 2023 | Accepted: 5 April 2023

DOI: 10.1002/vnl.22006

REVIEW ARTICLE

JOURNAL OF Vinyl & Additive TECHNOLOGY WILEY

Impact of physico-chemical properties of nanocellulose on rheology of aqueous suspensions and its utility in multiple fields: A review

Ashvinder K. Rana[1] | **Vijay Kumar Thakur**[2,3]

[1]Department of Chemistry, Sri Sai University, Palampur, India

[2]Biorefining and Advanced Materials Research Center, Scotland's Rural College (SRUC), Edinburgh, UK

[3]School of Engineering, University of Petroleum & Energy Studies (UPES), Dehradun, India

Correspondence
Ashvinder K. Rana, Department of Chemistry, Sri Sai University, Palampur, 176061 India.
Email: ranaashvinder@gmail.com; ranaashvinder2020@gmail.com

Vijay Kumar Thakur, Biorefining and Advanced Materials Research Center, Scotland's Rural College (SRUC), Kings Buildings, West Mains Road, Edinburgh, UK.
Email: vijay.thakur@sruc.ac.uk

Abstract

Nanocellulose (NC), due to its sustainable nature, high aspect ratio, superior mechanical strength, and availability of functionalizable —OH groups, has been widely utilized as reinforcement in numerous fluids/plastics. The physico-chemical properties of NC, like surface characteristics, dimensions/aspect ratio and their concentration, significantly impact the interparticle interactions, such as the extent of hydrogen bonding, van der *Waal* forces, hydrophobicity, electrostatic attraction/repulsion, and cellulose entanglement, and have been found to play a critical role in regulating the overall rheological characteristics of fluids. The functionalized NC aqueous suspension exhibited unique shear thinning properties, thixotropic behavior, and quick steady-state viscosity recovery and viscoelastic properties. However, upon adding functionalized NC to other fluids, a different impact was noticed. For instance, it improved the viscosity, G′ and mechanical stability of bio-ink; the setting time and mechanical strength of cementitious fluids; increased the filtration performance and provided a unique thermo-thickening impact in case of water-based drilling-fluid; enhanced viscosity with time and heat in case of oil recovery, and so forth. Keeping in view the notable dependence of the rheology of fluids on NC additives, in the present review article, the impact of various physico-chemical properties of NC additives on the rheological behavior of NC aqueous suspension and its utility as a rheology modifier in multiple advanced fields has been explored. This review article, compared to previous studies, warrants an update on the impact of recent NC surface functionalization/blending techniques employed and NC aspect ratio on specific properties of multiple advanced fluids.

KEYWORDS

3D-bio-printing, aqueous suspension, food additives, NC, post-processing, rheology

1 | INTRODUCTION

Due to the non-biodegradable nature of petroleum-based products, researchers have focused their attention on developing smart, high-performance, bio-compatible, biodegradable, and sustainable materials.[1–4] In this context, agricultural and forest residues are viewed as renewable natural resources.[5,6] Their significant potential for the creation of numerous engineered goods has been confirmed by the wide range of industrial activities related to paper, polymer composites, water purifiers, forest products, cellophane films, dietary fibers, and so forth.[7–11] The plants and trees have an essential basic reinforcing element called "cellulose," which endow these forest-based assets with tremendous strength and capabilities.[8,12,13] Further, the discrete hierarchical cellulose structure that spans from the macroscale to nanoscale dimensions opens the opportunity to investigate these plant-/trees-based materials at nanoscale dimensions[7,8,14–17] (Figure 1).

Conversion of cellulose microfibrils, which are composed of cellulose, lignin, and hemicelluloses, into nano cellulosic form is necessary for sustainable development involving nanotechnology in both industrial and research fields because of its alluring characteristics unlike conventional cellulosic products, including high surface area, outstanding mechanical qualities, abundant hydroxyl groups for surface functionalization, and bio-compatible nature.[18–20] The source of origin and processes applied for the extraction of nanocellulose (NC), have a significant impact on the surface morphology and various other properties of NC, including their percent crystalline nature, tensile strength, elastic modulus, thermal strength, colloidal behavior, liquid crystallinity, self-assembling properties, optical characteristics, and impermeability. Due to the abundance of hydroxyl groups, NC offers a simple and easily accessible platform for surface functionalization utilizing various physical and chemical techniques.[6,13,21] These techniques, in addition to providing solutions to many of the issues related to their practical uses, also enable the production of various NC-based high-value products. Over the past decade, NC has been used as templates, fillers or components in a wide range of emerging fields, such as in water treatment,[19,22,23] polymer composites,[24,25] food industry,[26,27] aerogels and hydrogels,[28] catalysis,[29] electronic and electrical industry,[6,30] and liquid crystal templates.[31]

Nowadays, the rheological properties of NC suspensions, such as their shear thinning behavior, yield stress, viscosity, viscoelasticity, and thixotropy, have received a lot of attention.[32–34] At a suitable concentration, NC produces a highly viscous aqueous suspension due to the prevalence of percolation interconnections/networks and chemical bonding/attractions (such as electrostatic repulsion and attraction, hydrogen bonding, van der *Waals* and hydrophobic attraction) along with entanglement. Continuous shearing of suspension causes NC to align itself with the flow direction, thus showing shear thinning behavior. Furthermore, NC suspension reverts at rest to their initial/original structure (thixotropic property), facilitating faster recovery of viscoelastic properties and steady-state viscosity. Due to their appealing flow

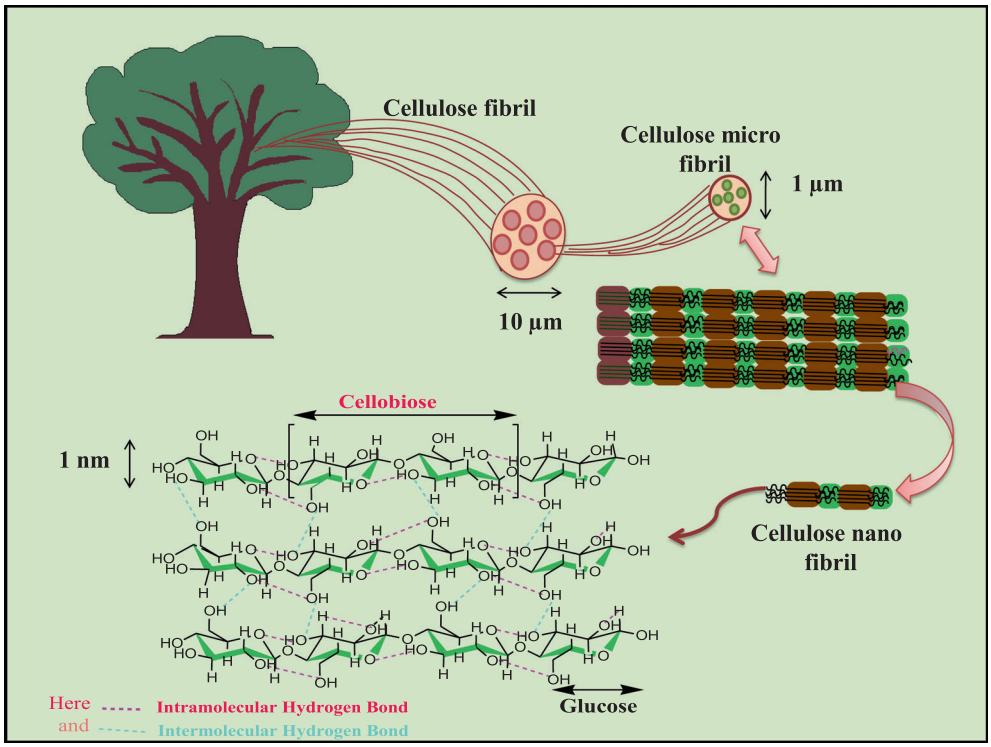

FIGURE 1 Schematic view of top-down cellulose hierarchical structure.

characteristics, NC can be utilized as efficient rheological modifiers in many applications.

Considering the huge potential of cellulose, the present review article has been focused on the summarization of its ability as a rheology modifier in a broad range of applications. No doubt, a couple of review articles have already been published mentioning the potential of NC as a rheology modifier and multiple factors such as time, temperature, shear rate, polyelectrolyte impact, and so forth, affecting their rheological behavior.[35,36] In their review article, Yadav et al.[28] focused on the procurement of nano cellulose from plant-based sources and its use in the biomaterial field as bio-ink for 3D bio-printing. On the other hand, Li et al.[29] in their review article, have detailed the cellulose nanomaterial's rheology dependence on test protocols along with its application in the fluid field.

However, in the current review article, endeavors have been made on a thorough examination of the effect of physico-chemical properties of nanocellulose additives on the rheology of NC in aqueous suspensions and its use in a variety of cutting-edge applications in the last 2–3 years, including bio-medical, food, oil, and polymer industries, and so forth, that have not been covered in the previous literature.

2 | SYNTHESIS AND COMPARATIVE VIEW OF PHYSICO-CHEMICAL PROPERTIES OF DIFFERENT TYPES OF NANOCELLULOSE

Depending upon dimensions and source of origin, NC can be categorized into three types, namely cellulose nanofibers (CNF), cellulose nanocrystals (CNCs) and bacterial NC (synthesized by bacteria)[37–39] (Figure 2). The former two, extracted from cellulosic materials such as plants, trees, seeds, agriculture wastes, nuts, and so forth, are of prime interest and are also thoroughly investigated in the present review. The intrinsic features like size, mechanical toughness, % crystallinity, and morphology of NC vary with the type of fibers and are also influenced by the type of extraction techniques employed or by the source of nanofibers.[13,19,22,40] The physico-chemical properties of two nano cellulosic forms, that is, CNCs and CNFs, which have been most preferably utilized as rheology modifiers in multidimensional applications, are discussed in Table 1. It can be inferred from the table that CNCs are denser, more crystalline, and have a superior aspect ratio than CNFs. Acid hydrolysis techniques generally synthesize CNCs. Commonly utilized acids are hydrochloric, sulfuric, phosphoric, and formic acids. The corresponding CNCs in the present article have been abbreviated as H-CNCs, S-CNCs, P-CNCs, and F-CNCs, respectively.

The acid hydrolysis technique removes selective amorphous cellulose regions and thus produces highly crystalline particles with source-dependent dimensions, for example, 5–20 nm × 100–500 nm for plant source CNCs.[13] Sulfuric acid, phosphoric acid hydrolysis and oxalic acid/2,2,6,6-tetramethylpiperidine-1-oxyl radical(TEMPO) oxidation lead to the grafting of negatively charged sulphate half-esters, phosphates and carboxylate groups onto the surface of the CNCs, which prevents the CNCs from aggregating in aqueous suspensions because of electrostatic repulsion between charged groups present on the NC. Additionally, the rod-like form of CNCs supports liquid crystals' concentration-dependent self-assembly activity. The effect of various parameters like temperature, time, acid concentration, and relative proportions of cellulose and acids on % crystallinity, surface chemistry, and % yield of CNCs have been investigated by numerous researchers.[41–45]

It has been observed that the proportion of sulphate groups on CNC surfaces increases with a rise in sulfuric acid concentration but is rarely affected by hydrolysis time. Additionally, low temperature promotes the existence of more sulphate groups, whereas high temperature may cause de-esterification and result in fewer sulphate groups. In contrast to the above study, the percentage of phosphate groups onto P-CNCs found to depend on temperature and hydrolysis timing only.[44] Similarly, the number of carboxyl groups onto TO-CNCs surface was also found to increase with the increase in temperature and time of reactions.[45] Additionally, it has been demonstrated that the acid hydrolysis process employed affects CNC thermal stability of CNCs. For instance, P-CNCs displayed better thermal stability than S-CNCs.

CNFs, unlike CNCs, are comparatively long (micrometers in length) and contain both crystalline cellulose and amorphous regions.[46] The intertwined long CNFs produce highly viscous aqueous suspensions at comparatively low concentrations (<1%). Three different techniques, namely mechanical treatments (such as milling, grinding and homogenization), chemical treatments (TEMPO oxidation, carboxymethylation, sulfonation, etc.); and chemical/enzymatic pretreatments followed by mechanical disintegration can be used to extract CNFs from cellulosic materials.[36,46–48] In the present article, CNFs synthesized through pretreatment steps of sulfonation, enzymatic, TEMPO oxidation, periodate-chlorite oxidation, and carboxymethylation prior to mechanical deterioration have been designated as S-CNFs, E-CNFs, TO-CNF, PC-CNFs and CM-CNFs respectively. Here, chemical pretreatments, in addition to controlling the CNFs morphology, also change its surface chemistry and charges.

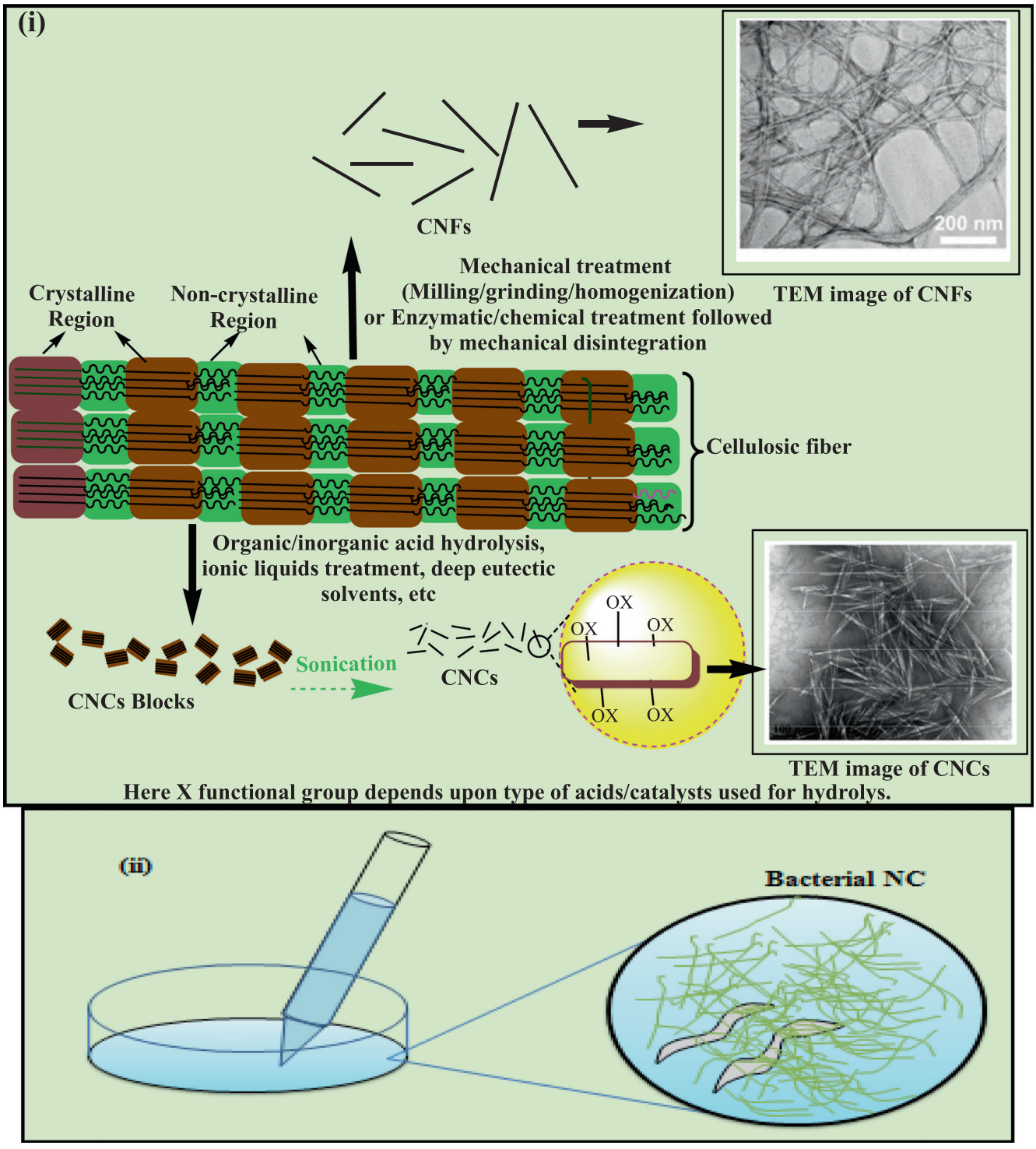

FIGURE 2 Schematic view of the formation of (i) CNCs and CNFs, and the TEM images of CNCs extracted from wood pulp using enzymatic technique and CNFs prepared from bleached softwood sulfate pulp.[37–39] (TEM images of CNCs and CNFs reprinted from Refs. [37,38] respectively, under creative common license CC BY license, MDPI publisher) and (ii) bacterial NC.

3 | NANOCELLULOSE-FLUID RHEOLOGY

NC suspensions exhibit very complex flow behaviors because of the complex surface chemistry and morphology of NC. Other researchers have already discussed the detailed analysis of its flow nature,[28,29,36] so here we will be precisely explaining its role. The aqueous suspensions of CNCs and CNFs cellulose show lyotropic phase behavior and flocculation behavior, respectively. On increasing the shear rate, CNC and CNFs exhibit shear thinning behavior and gradually align along the flow direction. The

TABLE 1 Extraction techniques, dimension, mechanical strength, % crystallinity and characteristics of NC extracted from plants/agriculture wastes.

Nano cellulose type	Synthesis techniques	Dimension	Density (g/cm^3)	Tensile strength and Young's modulus	% crystallinity	Characteristic	References
CNFs	Generally synthesized from cellulose using mechanical treatment. However, to lessen the energy requirement cellulose may be chemically or enzymatic ally pre-treated. Most commonly utilized chemical pretreatments are TEMPO, cationization carboxymethylation, periodate-chlorite oxidation, sulfonation.	Diameter: 1–100 nm; Length: 500–2000 nm High aspect ratio	1.5	Young's modulus: 30 GPa Tensile strength: 357.5 MPa	45%–80%	Bio-degradable, bio-compatible, good water retention tendency	[13,19,22,49]
CNCs	Enzymatic hydrolysis, organosolv treatment, organic/inorganic acids, ionic liquids, deep eutectic solvents, TEMPO-oxidation, mechanical methods, etc. may be employed to extract CNC from precursor cellulosic molecules	Length: 100–500 nm; Diameter: 2–20 nm High aspect ratio (~70)	1.6	Tensile strength: 7500–7700 MPa; Young's modulus: 120 GPa	54%–88%	Highly crystalline compared to CNFs, mechanically quite strong, good bio-degradability and bio-compatibility; better water retention ability	[13,19,22,49]

flocculation of CNF, lyotropic phase of CNCs, and shear-induced orientation behaviors are critically relevant for their rheological properties.

Fluids are generally of two types, namely Newtonian and non-Newtonian fluids (Figure 3A,B). Newtonian fluids show constant viscosity; adding a dispersed phase to them may lead to numerous non-Newtonian behaviors of the resulting fluids, that is, shear-thinning (pseudo-plastic), shear thickening, Bingham plastic, and Bingham pseudoplastic.[36] The shear-thinning fluids exhibit a gradual decrease in viscosity with an increase in shear rate. Contrary to this, in shear-thickening fluids, the viscosity of fluids increases with an increase in shear rate. Bingham plastic fluids behave as rigid solids below the yield stress, above which these fluids obey Newtonian fluids behavior. Bingham pseudo plastic fluids, just like Bingham plastic fluids, also exhibit a yield stress, but above the yield stress, they show shear-thinning behavior.

Further, thixotropic and rheopectic fluids also come under the heading of Non-Newtonian fluids. Thixotropic fluid is a time-dependent shear thinning fluid, while rheopectic fluid is a time-dependent shear thickening fluid. That simply means the former becomes less viscous and the latter more viscous or even solidified over time when sheared, agitated, or shaken.

The viscoelastic behavior of NC suspensions can be studied by measurement of change in oscillatory shear as functions of strain, γ, (strain sweep) and frequency, ω, (frequency sweep). In the linear region, the strain sweep curve of CNC suspensions showed stable storage modulus (G′) and loss modulus (G″) (Figure 3C). However, above a critical strain value (γc), a nonlinear region appears in which the dynamic moduli vary as a function of the strain, and in most cases, they decrease with an increase in strain.[50] The shape of the frequency sweep curve depends on the properties of viscoelastic materials. For solid viscoelastic materials, G″ varies linearly,

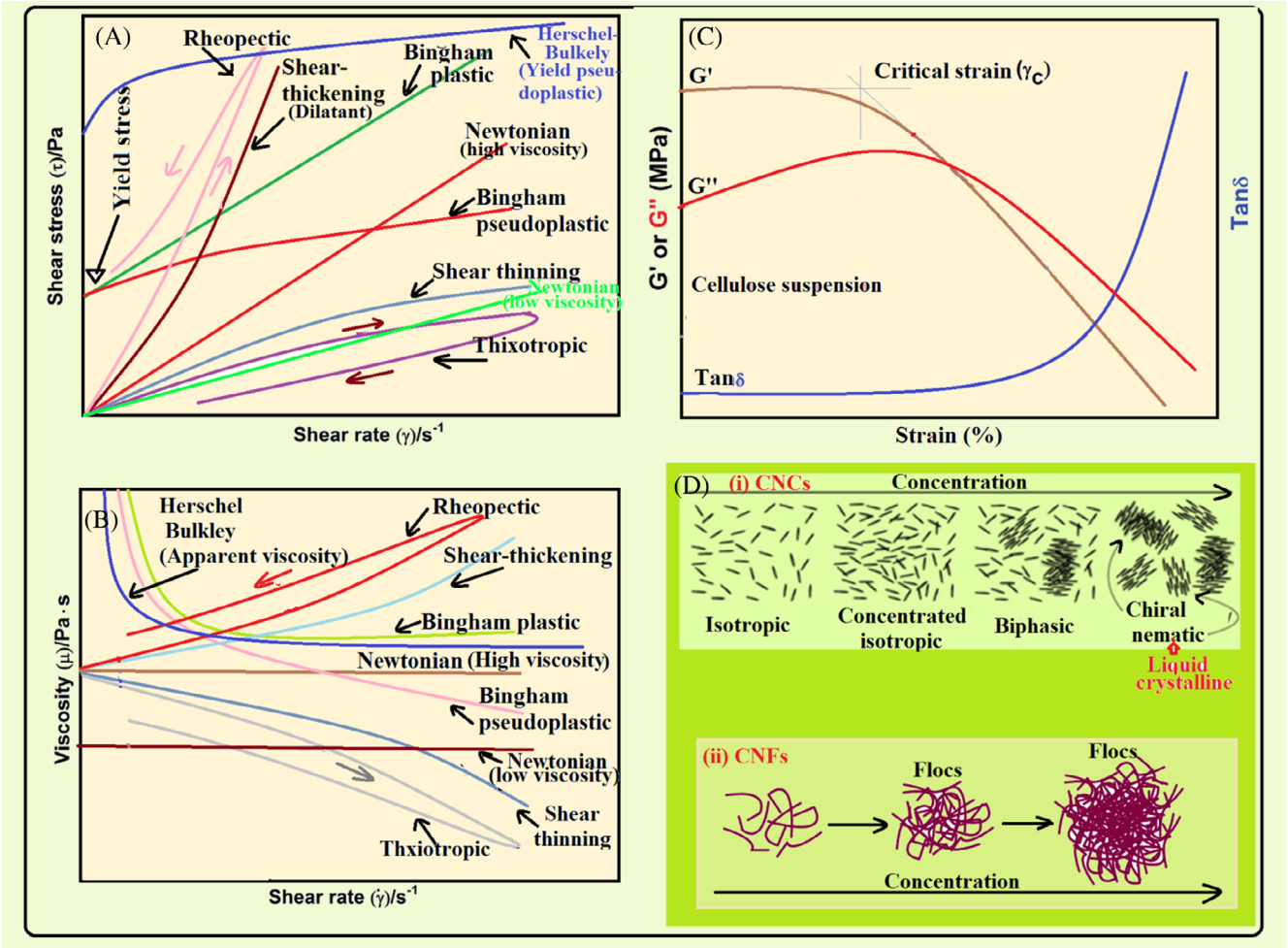

FIGURE 3 (A) Shear stress, (B) viscosity curves versus shear rate (C) viscoelasticity versus strain for different types of fluids and (D) self assembly of CNCs and CNFs with increase in their concentration in aqueous suspension.[36,51] (A part of the Figure has been adapted from Ref. [51] Copyright {2021} American Chemical Society).

whereas G′ remains independent of the frequency; in the case of gel-like materials, both G″ and G′ remain independent of the frequency; for the viscoelastic liquids, both G″ and G′ increase gradually with the enhancement in frequency.

Rheological characteristics of fluids depend upon time, temperature, shear rate and the physicochemical properties of dispersed particles. Aspect ratio and shear rate are two governing factors in the case of rod- and fibril-like NC.

4 | IMPACT OF PHYSICO-CHEMICAL PROPERTIES OF NANOCELLULOSE ON THE RHEOLOGY OF AQUEOUS SUSPENSIONS

Contrary to previous review in this sector,[36] extensive analysis of the NC aspect ratio extracted from various bio-sources, the effect of crowding factor in determining overall rheology and the influence of several advanced graft copolymerization/functionalization procedures such as polyethyleneimine grafting, azetidinium salts grafting, copper bromide and polyvinylcaprolactum modification, and so forth, on rheology of NC suspension have been reviewed in present paper.

4.1 | Rheology of cellulose nanocrystals suspension.

Surface chemistry and the aspect ratio of CNC are the crucial physicochemical parameters that govern the concentration-dependent lyotropic phase formation of CNC suspensions.[52,53] The impact of the physicochemical properties of CNCs on the rheology of aqueous suspension has been discussed below.

4.1.1 | Rheology variation with concentration

Due to smaller dimensions and a moderate aspect ratio, CNCs, in comparison to CNFs, align themselves more readily along the direction of shear, thus considerably impacting the rheology characteristics of CNC suspensions. It has been observed that with a gradual enhancement in CNC concentration, their dispersion readily undergoes a transition from isotropic to biphasic phase, comprising both liquid crystalline and isotropic, to fully liquid crystalline and finally to gel form (Figure 3D (i)).

Urena-Benavides et al.[53] have confirmed the generation of biphasic, liquid crystalline phase, and gel with the increase in CNC concentration using polarized optical microscopy (POM). They reported that the transition from isotropic to biphasic phase for S-CNC (extracted from cotton) suspensions took place when concentration was increased upto 4.5, 4.05 and 4.2 wt.% at 45°, 20°, and 4°C, respectively. However, upon a further increase in CNC concentration, the transformation from biphasic to entirely liquid phase and finally to gel has been demonstrated by them. Their results were found to be consistent with the finding of Dong et al., who introduced the term "critical concentration" for a change in phase.[54] Bercea and Navard have confirmed the first birefringent liquid crystalline domains in S-CNC suspension at a very low 0.8 wt.% by employing crossed optical microscopy technique.[55] The transformations from a dilute to a semi-dilute and finally to a concentrated regime have been confirmed utilizing the rigid rod approximation technique at a volume fraction of f^{-2} and f^{-1}, respectively.

Various techniques have been utilized to confirm the orientation of CNCs under shear stress, such as small angle light scattering (SALS),[56] small angle neutron scattering (SANS),[57] small angle X-ray scattering (SAXS),[58] SEM[59] and POM[60] observations.

Shafiei-Sabet et al.[60] studied the impact of ultrasound energy (ranging from 0–5000 J/g CNCs) by employing a polarized optical microscopy technique on rheological properties of 5 and 7 wt.% CNCs suspensions. They reported that ultrasound energy impacts the microstructure of CNCs suspension, and their suspension shows gel-like behavior before sonication; however, they reported shear thinning behavior after sonication. Viscosity has been noticed to drop significantly in three different regions typical to that of lyotropic liquid crystals. In region I, alignment of the chiral nematic liquid crystal domains take place, which is then followed by a plateau region (II region), where the domains orient themselves along the direction of shear stress and finally region III, which involves destruction of liquid crystal domains at higher shear stress leading to orientation of individual nano rods along shear stress.

When nano crystalline cellulose (S-CNC) was varied from 1 to 11.9 wt.% concentration, a significant enhancement in the viscosity of suspensions was observed due to the formation of a complex/strong network between NC[61](Figure 4A,B). Further, at low concentrations, up to 3 wt.%, nano cellulose suspensions showed near-Newtonian behavior, that is, very low shear thinning behavior and power-law ($G' = kC^n$; k represents fibers characteristics and value of n indicates the concentration-dependent network of NC suspensions) response between shear stress and shear strain with exponents of between 0.91 and 1. Here, a higher 'n' (power law-exponent) value indicates more dependence on the concentration of the cellulose network. However, when NC concentration was varied from 4–7 wt.%, suspensions showed a slight shear thinning behavior at a low shear rate. Shear thinning becomes quite significant at a higher shear rate, with 'n' values decreasing from 0.74 (4 wt.%) to 0.29 (7 wt.%). On further increase in the concentrations to 11.8 wt.%, the samples showed strong shear thinning power law behavior with 'n' values approaching zero, which is the property of a yield stress fluid. This behavior has been attributed to the formation of closely packed structures, resulting in poor particle motion at higher cellulose concentrations.[53,62]

Contrary to the above results, Shahabuddin et al.,[63] in their study, while evaluating the impact of S-CNCs and P-CNCs concentrations (varied from 1–5 wt.%) onto their rheological properties, found no Newtonian plateau region(Figure 4C,D). They reported a shear thinning behavior for all samples at varying shear rate. Further, among S-CNC and P-CNCs, the later was reported to have higher viscosity owing to the presence of a higher number of hydroxyl groups on the S-CNCs surface, resulting in better interaction of S-CNCs with water molecules, which in turn increased the hydration forces and thus lowered the viscosity.[64]

Isotropic behavior, that is, shear thinning at lower shear rates and Newtonian behavior at intermediate and higher shear rate was demonstrated for CNCs suspended at 1 wt.% concentration. However, when concentration was increased from 1 wt%.[65] or CNCs is catinocally modified, then the viscosity of suspension was noticed to vary in three regions (shear-thinning followed by shear thickening and again shear thinning). Further, for cationically modified samples, gel formation was noted for samples at both 1 and 2 wt.% suspensions, which has been confirmed through dynamic viscoelasticity study, showing differences in storage and loss modules, that is, $G' > G''$.

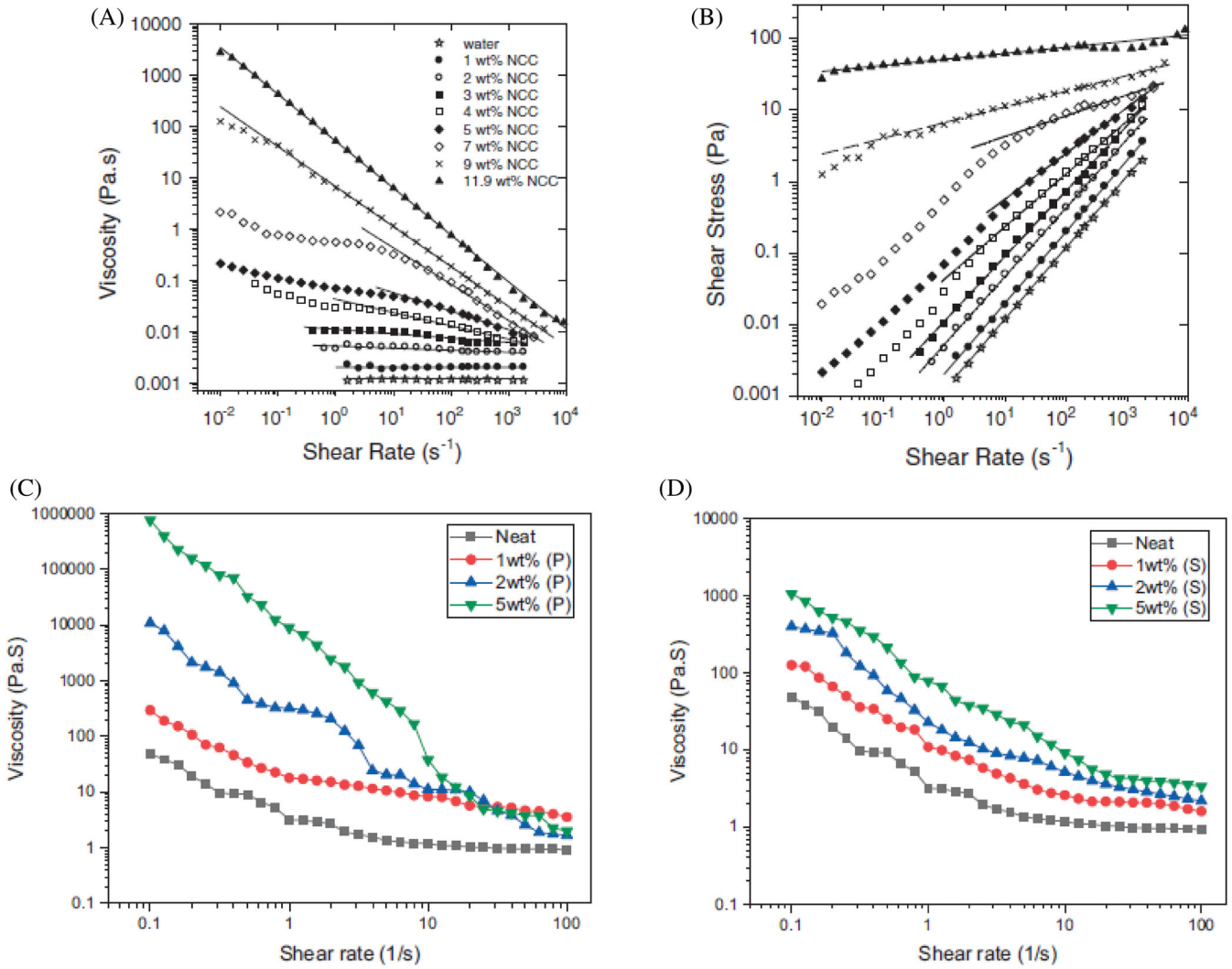

FIGURE 4 Rheology of CNCs suspensions in water, (A) apparent viscosity versus shear rate for S-CNC suspension (1–11.9 wt.%), (B) shear stress versus shear rate for S-CNC. Here solid lines represent the power law fits to regions of the flow curves.[61] ("Figure A and B reprinted with permission from Ref. [61]. Copyright {2017} Elsevier.") (C) viscosity versus shear rate for P-CNC (1–5 wt.%) and (D) viscosity versus shear rate for S-CNC (1–5 wt.% suspension) ("Figure C & D reprinted with permission from Ref. [63]. Copyright {2022} Elsevier.").

4.1.2 | Rheology variation with dimensions/ aspect ratio of cellulose nanocrystals

The rheological characteristics of NC suspensions were found to largely depend upon the size of the nanomaterials and infact noted to be directly proportional to aspect ratio and their dispersion microstructure.[36] A couple of research articles[56,61,64,66–72] have been reported on the dependency of rheological characteristics on the aspect ratio of CNCs.

Since the aspect ratio or dimensions of CNCs can be easily determined using TEM and AFM techniques, their impact on rheological properties can be easily co-related. For 1 wt.% suspension of CNCs having an aspect ratio greater than 35, in addition to high viscosity at a lower shear rate, a shear thinning behavior with an increase in shear rate was observed (shear rate varied from 10^{-1} to 10^{3}). However, for CNCs with an aspect ratio less than 35, Newtonian behavior and shear thickening or shear thinning were observed in the shear range 1 to 1000 s^{-1} and 10^{-1} to 1, respectively. The variation in viscosity of CNCs over the range of 10^{-3} to 10^{2} Pa with the variation in aspect ratio allows CNCs to be utilized as rheological modifiers in a wide range of commercial applications.

Babaei-Ghazvini and Acharya[73] studied the impact of aspect ratio of CNCs extracted from club tunicates (TCNC: 65 aspect ratio) and wood (WCNC: 15 aspect ratio), and their hybrid mixtures (HCNC: TCNC +WCNC) on the rheology of resulted CNC suspension (Figure 5A). A strong co-relation between average viscosity of CNC suspension (at 1 wt.%) and aspect ratio of CNCs has been confirmed by them. When compared at

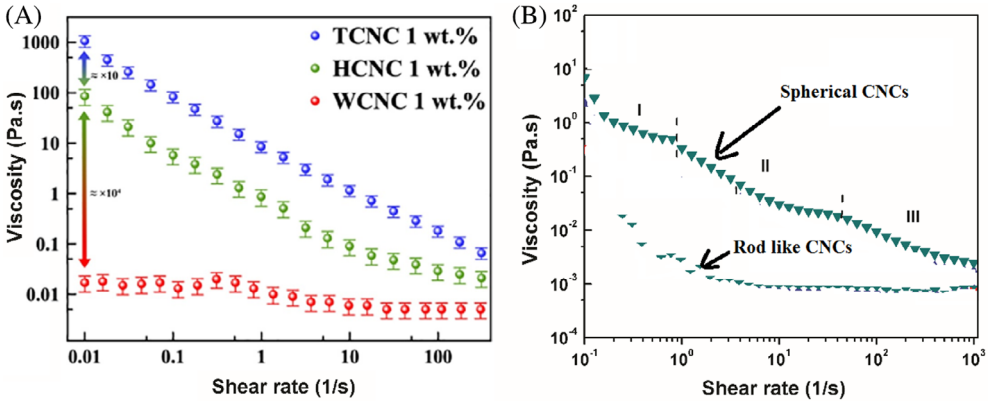

FIGURE 5 Steady-shear viscosity of (i) 1 wt% TCNC, HCNC, and WCNC suspensions and (ii) 1.5 wt.% spherical and rod line CNCs suspension. ("Figure 'a' reprinted from Ref. [73]. Copyright {2022} Elsevier Creative Commons CC-BY-NC-ND" and "Figure 'B' reprinted with permission from Ref. [64]. Copyright {2017} Elsevier.")

same shear rate, TCNC showed maximum viscosity of 1063 Pa s followed by HCNC (85 Pa s) and WCNC (0.02 Pa s). The higher viscosity of TCNCs in comparison to WCNC has been related to stronger TCNCs interparticular interactions because of higher aspect ratio, which in turn has led to increased interparticle hydrogen bonding and thus higher viscosity for TCNC than WCNCs. Further, both TCNC and HCNC suspensions were found to exhibit non-Newtonian shear-thinning behavior, but contrary to it, WCNC suspension showed Newtonian flow behavior. The XRD analysis revealed that WCNCs films were unable to maintain the anisotropic effect in their structure and form chiral nematic structures in response to shear forces. However, at the same concentration, HCNC and TCNC films showed anisotropic characteristics. Zhou et al.[64] also confirmed an increase in the viscosity of CNCs suspensions (0.25–1.5 wt.%) with an increase in an aspect ratio of nanoparticles. Figure 5B displays the comparative view of viscosity for spherical and rod-like CNCs at 1.5 wt.% suspension. As the aspect ratio of nanocrystals increases from 1 (rod-like CNCs) to 5–25 (spherical CNCs), the viscosity of suspension also increases. From the data above, it can be inferred that aspect ratio (length/diameter) has a significant impact on the rheology of CNCs suspension, and as a result, extreme caution should be used while choosing the extraction method for CNCs from waste biomass.

4.1.3 | Rheology variation with surface functionalization/extraction technique employed

The type of charge, its density, functional groups, and hydrophilic and hydrophobic nature of functional groups grafted onto surface NC plays a crucial role in controlling the rheology characteristics of NC suspension by altering physical and chemical interactions among neighboring CNCs or CNFs. With diverse surface chemistry, NC can be created by employing different isolation/production methods or surface functionalization techniques. The repulsive or attractive forces between NC, depending on the contiguous geometry of fortifying particles within the mixture, impact the overall rheological properties of suspension.[74] The contiguous geometry of particles causes an increase in the yield stress,[75] whereas when multiparticle geometry is broken or discontinuous, overall interaction among particles can result in a reduction in viscosity.[76] The impact of different NC isolation and surface modification techniques on the rheological properties of their suspensions has been summarized in Table 2.

Contrary to CNFs, for CNCs, a decrease in viscosity and G′ was noticed with an increase in charged functional groups density. This behavior has been attributed to the better dispersion of CNCs because of diminished chemical interaction among CNCs and increased electrostatic repulsion between similarly charged CNCs.[63,77,78] The rheological characteristics of synthesized CNC can be tailored by various surface modification techniques such as desulfonation[79] and hydrophobization,[80–84] which impact the rheology characteristics of CNCs according to the type of charge or hydrophilic or hydrophobic nature.

For S-CNC, with increases in sulphate group contents from 0.27 to 0.49, and 0.57% and 0.89%, a significant decrement in the viscosity of samples was observed.[77] Shafiei-Sabet et al. also observed similar results upon increasing the degree of sulfation on CNCs.[78] However, some authors have reported results opposite to Shafiei-Sabet et al. They found an increase in viscosity with an increase in sulphate contents and demonstrated that this behavior might depend upon the type of equipment used for measurement of rheometry (capillary rheometer or more typical shear rheometer). Further, an increase in viscosity was noticed after the hydrophobization or desulfation of CNCs. This behavior has been attributed to the self-aggregation of hydrophobic CNCs in suspension.[79–84]

TABLE 2 Impact of different surface functionalization techniques onto rheology of CNC and CNF suspension.

Type of isolation/ treatment technique employed	Impact on G′	Impact on viscosity	Yield stress	Reason	References
(i) CNCs					
S-CNC		A 2 to 3 order of magnitude decrease in viscosity was noticed when the sulfate charge increases by ∼0.6		As sulfate contents increases it makes the suspension more stable because of repulsion between similar charged nano crystals	[77]
S-CNC	At 6.65 sulfur contents, G′ as well as G″ for S-CNC were found to be higher than 0.85 sulfur contents carrying S-CNC. Further at 7 wt.%, G″ was noticed to be >G′	When degree of sulfur contents increased from 0.69 to 0.85, a decrease in the viscosity was observed	—	Higher surface charges results in an increase in electrostatic repulsion, which leads to a lower probability of aggregation	[78]
Octyl-CNC: S-CNCs were converted into Octyl-CNCs by two step process, that is, oxidation of S-CNCs using periodate succeeded by the reductive amination using octylamine.	G′ for the octyl-CNCs gel (4300 Pa; at 5 wt %) was found to be higher than S-CNCs (0.05 Pa)	Significant enhancement in the viscosity after hydrophobization (Octyl-CNCs) of S-CNCs was observed	—	Hydrophobic interactions results in increased viscosity	[80]
Sulfuric acid hydrolysis	—	Noticed to decrease with an increase in sulfur contents onto CNFs from 0.27 to 0.89 S		Viscosity decreases due to better repulsion between similar charged nano crystals	[77]
Copper bromide and polyvinylcaprolactum modified CB-CNC and PVCL-CNC were prepared from sCNC utilizing ATRP technique	G′ increased after the hydrophobization of CNCs	Viscoelastic properties increased after chemical modification of CNCs		Transition from hydrophilic character to hydrophobic Causes enhanced gelling properties due to hydrophobic interactions among CNCs	[81]
Hydrothermal desulfation of S-CNC at varying temperatures (60-120°C)	Desulphation resulted in enhancement in removal of sulphhate contents from sCNCs with increase in treatment timing and ultimately increased the G′	Through dynamic viscoelastic studies, the transition from liquid to gel has been found to be in between 70 and 80°C. On further enhancement in the temperature, remarkable		The hydrothermaldesulfation resulted in the removal of sulfate groups and thus caused an increase in viscosity	[79]

TABLE 2 (Continued)

Type of isolation/ treatment technique employed	Impact on G′	Impact on viscosity	Yield stress	Reason	References
		enhancement in viscosity was noticed.			
Azetidinium salts grafted onto S-CNC	Increases after grafting of salts	The viscosity of CNC suspension increases after the grafting of salts	—	The increase in viscosity has been associated with an increase in hydrophobic interactions between the grafted CNCs	[82]
Polyethyleneimine (PEI) non-covalent grafting onto S-CNC	Freshly prepared 3% (w/w) PEI-CNC suspensions showed G′ similar to that of 3% (w/w) S-CNC suspension at the initial stage; however, with time, G′ of functionalized CNCs showed increase by about three decades over 20 h	The viscosity of CNC suspension increases after the surface modification of salts. Further, the Newtonian behavior of 3% (w/w) CNC suspension changed into a non-Newtonian gel system after surface functionalization	—	Functionalization lead to the enhancement of hydrophobic character onto functionalized CNCs	[83]
2,2,3,4,4,4-hexafluorobutyl methacrylate graft copolymerization onto HCl hydrolyse CNCs via ATRP technique	Addition of functionalized CNCs in oil suspension results in improved thixotropy and enhanced G′ and G″ .	Viscosity increases after surface functionalization because of development of hydrophobic character onto the CNC surface after fluoro polymer grafting	—	The self-aggregation, due to surface-coated hydrophobic fluoropolymer, was more serious in case of grafted CNCs.	[84]
Sulfuric acid and phosphoric acid utilization for production of S-CNC and P-CNCs	S-CNC showed higher G′ than P-CNC in aqueous suspension	At 5 wt%, P-CNC showed higher viscosity (772 800 Pa S) than S-CNC suspension (1045 Pa S)		The higher viscosity of P-CNC suspension than S-CNCs in an aqueous medium has been assigned due to the presence of more hydroxyl groups onto S-CNCs surface and has been confirmed with the help of FTIR study	[63]
(ii) CNFs					
TEMPO-oxidation	Noticed to be enhanced when carboxyl content onto TO-CNF increases from 0.25 to 0.45, 0.55, and 0.65 mmol/g	Increases with increase in carboxyl contents		However, upon a further increase in surface charge, the electrostatic repulsion forces among nanofibrils and aspect ratio becomes	[114]

(Continues)

TABLE 2 (Continued)

Type of isolation/ treatment technique employed	Impact on G′	Impact on viscosity	Yield stress	Reason	References
				dominant, which in turn lowers G' as well as viscosity	
Carboxymethylation followed by mechanical grinding	Carboxyl group contents increases from 0.01 to 1.14 mmol/g, when reaction time was varied from 30 to 90 min. Both shear and G′ noticed to be increased with increase in cabxoyl group contents (Figure 6)	Increases with increase in the carboxyl group (measured at 0.75 wt.% CNF concentration)(Figure 6)	Enhanced from 1.7 to 10.6 Pa as the carboxylic content increased from 0.01 to 1.14 mmol/g	As carboxyl group contents increase, it makes the gel of CNFs more stable because of better repulsion between nanofibrils	[115]
TEMPO oxidation followed by high-intensity ultrasonication Sample code: TO-CNFs	Increases as the surface charge or carboxyl contents increased from 0.659 to 0.879 and 1.24 mmol/g	Noticed to be increased with increase in surface charge and time of HPH	Yield stress increased with increase in mechanical disintegration times	The better will be individualization of CNFs, the more crossed-network formation between nanofibers can be achieved	[113]
Periodate–chlorite oxidation followed by HPH Sample code: TO-CNFs	—	The carboxyl contents were noticed to increase from 0.38 to 0.69, 0.75, 1.20 and 1.75 mmol/g with increase in oxidation time from 15 to 30, 60, 120 and 180 min. Interestingly, viscosity of PC-CNFs increases with increase in carboxyl contents and was found maximum for suspension having 1.20 mmol/g carboxyl contents. However, on further increasing in carboxyl contents (1.75 mmol/g), viscosity diminishes.	—	The low aspect ratio and strong electrostatic repulsion force become dominant at high carboxyl contents (1.75 mmol/g), leading to a reduction in viscosity.	[116]

4.2 | Rheology of cellulose nanofibers suspension

4.2.1 | Rheology variation with cellulose nano fibers concentration

CNF, due to stiff inter-fibrillar interactions, becomes highly entangled and thus forms floccules (Figure 3D (ii)). The formation of flocs and shear-induced orientation of CNF control the rheological properties of CNF suspensions at steady shearing and rest conditions.

Different physical techniques such as optical coherence tomography,[85,86] photoelastic modulator,[87] digital imaging,[88,89] ultrasonic speckle velocimetry[90] and magnetic resonance imaging velocimetry[91] have been utilized by different researchers to monitor the microstructure changes of CNF during shear rheology evaluation. With the help of an optical coherence tomography device in combination with a pipe rheometer[85] or rotational rheometer,[86] it has been confirmed that highly elongated flocs flow along the shearing direction below the yield stress and above the yield stress flocs become almost spherical. The size of spherical flocs was noticed to be monotonically reduced when shear stress was further increased. Karppinen et al.[89] and Saarikoski et al.,[88] during their study on the relationship between rheological characteristics and microstructure of UN-CNF flocs by using digitally imaging technique (in transparent and cylindrical test geometry) found that microstructural variations of flocs largely depends upon changes in shear stress with enhancement in shear rate. Shear induced orientation of fibrils in TEMPO oxidized-CNF suspension was confirmed utilizing photo-elastic modulator (having a parallel plate geometry), and have been found to be have parallel alignment along the flow direction when shear rate was in intermediate range (30–40 s^{-1}).[87] Further, the two dimensional spatial and time-resolved characterization of the shear flow of E-CNF and TO-CNF suspensions was done with the help of ultrasonic speckle velocimetry technique.[90] For E-CNF in comparison to TO-CNF suspensions, spatial velocity map was noticed to be very erratic confirming presence of flocs in the E-CNF suspension and absence of mesoscale flocs in micrometric scale in case of TO-CNF. The difference in flocs behavior of two types of CNF has been attributed to presence of highly charged surface onto TO-CNF, which leads to homogenous dispersion.

Switzer and Klingenberg[92] demonstrated that the fiber flocculation directly influences the rheological characteristics of the fiber suspension and is supposed to initiate above a certain threshold concentration of fibers, where fibers come into continuous contact in a network structure with each other. To parameterize the number of contacts between the fibers based on aspect ratio and concentration, Kerekes and Schell defined a crowding factor (N), which means a number of fibers having a spherical volume of diameter equal to the fiber's length.[93]

$$N = 2/3\phi\left(l/d^2\right) = 2/3\phi A^2.$$

Where, ϕ, l, d and A represent the concentration, length, diameter and aspect ratio of the fibers, respectively. When N lies less than 1, that means flocculation does not occur, that is, each fiber can rotate freely to the other. However, when the value of $60 < N$, then fibers form a connected network with each other and show no mobility of individual fibers. However, in the range $60 > N > 1$, nil possibility of a connected network has been reported, but fibers in this range may form flocculate because of shear-induced rotation as well due to the creation of flocs.[93,94]

However, in the case of CNF suspensions, one should take into account the polydispersity of the fiber length when estimating the crowding factor. In the case of CNFs, a number of contact points are possible, which may lead to an underestimation/miscalculation of the crowding factor. Kropholler and Sampson[95] applied the following correction term to the crowding factor in order to account for this.

$$N' = N\left(1 + CV^2\right)^4.$$

Here N′ is the corrected crowding factor, and CV is the coefficient of variation (related to the polydispersity) and is calculated by dividing the standard deviation of the length distribution with the average length value.

Wang et al.,[96] during their steady of shear thinning behavior of varying amounts (0.1 to 1.0 mg/mL) of low and high-charged TO-CNFs suspension, reported a corrected crowding factor (N′) ≈ 14 at overlap concentrations, that is, 0.52 and 0.33 mg/mL in case of low and high charged CNFs, respectively. They demonstrated a dilution regime for suspension at $N' < 14$ and semi dilution regime at $N' > 14$. At higher charges, the length of CNFs remains the same, but the aspect ratio increases because of decrement in cross-section dimensions, which in turn leads to a larger value of N′ for densely charged CNFs. Further, an exponent value of 1.2 and 3.4, and 1.0 and 2.8 was noticed for low- and high-charged TO-CNFs below and above the overlap concentrations, respectively. Contrary to Wang et al., a couple of researchers reported a broad range of exponent values for TO-CNFs, for example, 2.5,[97] 3,[98] 4.6,[99] and 4.62[100] for TO-CNFs. Contradictory to the above results,

Wang et al.,[101] in another study, demonstrated a crowding factor value of 16 for CNFs suspension and reported that this variation might be because of the different parent sources of the CNFs, inconsistencies in the pretreatment applied, resulting in fibers of different dimensions, crystallinity, and fiber flexibility. Further, exponent values for enzymatically extracted CNFs and CM-CNFs were reported to be 3.3[102] (extracted from kenaf pulp) and, 2.5[103] and 5.2,[76] respectively.

A couple of researchers reported an increase in suspension viscosity with an increase in CNF concentration.[67,104,105] Wang et al.[104] reported typical shear thinning behavior for CNF suspensions. When the shear rate was varied from 0.01 to 1000 s^{-1}, the suspension displayed high viscosity at a very low shear rate due to the entangled network of nanofibers; however, at higher shear rates, low viscosity was reported because of the deformation of the fibril structure. When the concentration of CNFs was increased beyond 0.5 wt.%, all samples showed different viscosity-decreasing trends with an increase in shear rate. Further, when the shear rate was kept constant, a continuous increase in viscosity with an increase in concentration was noted. Thus, we can conclude that dimensions as well density of surface charge, significantly influence the exponent value.

4.2.2 | Rheology variation with dimensions/aspect ratio of cellulose nanofibers

Source and production techniques play a significant role in controlling the dimensions or surface morphology of NC. Wang et al.[104] developed different types of CNFs samples from bleached hardwood kraft pulp by using SMC wall milling alone or in combination with pre- or post-endoglucanase enzymatic treatment for different times. At a very low shear rate (0.1 s^{-1}), three different samples, that is, CNFs prepared FiP1(synthesized from fine milling of cellulose pulp for 1 h; diameter:66 nm), Po-P1E1t3 (fine milling followed by enzymatic treatment for 3 h; diameter: 35 nm), and PoP1E1t48(fine milling followed by enzymatic treatment for 48 h; diameter: 29 nm) at a concentration of 0.5 wt.% showed distinct viscosities; noted to be higher for FiP1 followed byPo-P1E1t3 and PoP1E1t48. Such a difference in viscosities was noted to disappear when the shear rate was increased beyond 0.1 s^{-1}, and was found to almost disappear when the shear rate was >30 s^{-1} (shear rate was varied up to 1000 s^{-1}). The purpose of using different treatments either alone or in combination was simply to reduce the diameter of CNFs. The greater the diameter or polydispersity index (PDI) more will be the viscosities at a low shear rate. The higher viscosities for FiP1 compared to other samples could be due to aggregation and intertwining of large-sized fibrils with each other to form a more stable network structure.[106–108] From the above discussion, it can be noticed that enzymatic treatment plays a significant role in CNFs fibrillation. The relationship between the aspect ratio and the intrinsic viscosity can be best explained utilizing the Simha model, which clearly highlights the role of NC morphology on the rheological characteristics of NC suspensions. For E-CNFs, the G′ was noticed to decrease with the increase in dosage of enzyme treatment.[109] Further, CNFs with weaker networks were noticed to form with Celluclast 1.5 L (mixture containing exo-glucanases, endoglucanases, β-glucosidases and cellobiohydrolases) in comparison to Fiber Care R enzyme (endoglucanase).[48]

The untreated CNFs suspensions, prepared by grinding for an increased number of time followed by high-pressure homogenization (HPH) treatment (up to 5–8 passes), similar to enzymatic treatment, resulted in a decrease in the degree of polymerization or causes a decrease in the degree of fibrillation, which in turn yielded a better CNF network; however, in this case, higher viscosity of the suspension was found (at a shear rate of 100 s^{-1}) when the number of passes of pulp (from which CNFs were synthesized) through the grinder or

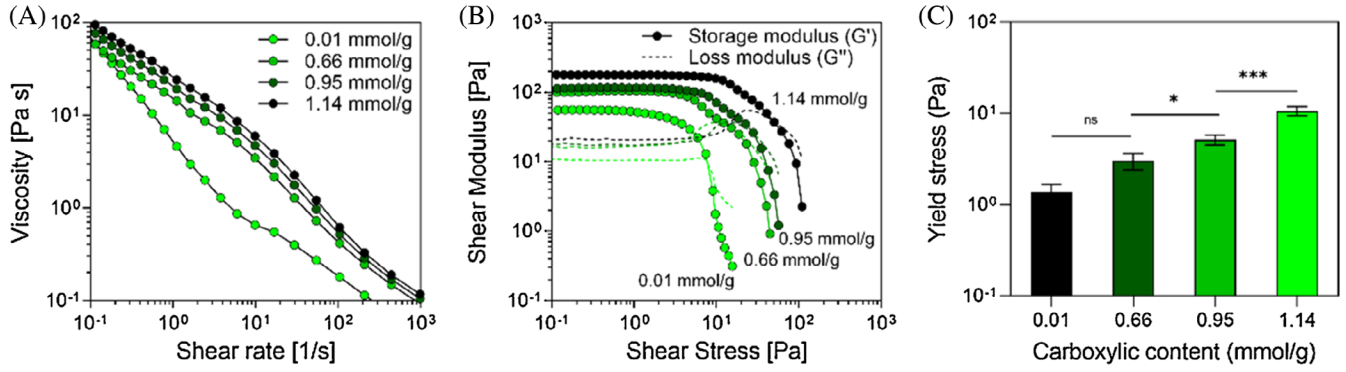

FIGURE 6 Variation in viscosity (A), storage modulus (B) and yield stress (C) with increase in carboxyl group contents.[115] "Reprinted with permission from Ref. [115]. Copyright {2021} Elsevier."

TABLE 3 The potential of CNFs as rheology modifiers in multiple fields.

Field of application	Application	Treatment applied onto NC	Remarks/conclusion	References
Electronic industry	Preparation of bio-based 3D-printable, conductive bio-ink to print electrical components and other devices.	CNFs were mixed with poly (3,4-ethylene dioxythiophene) poly(styrene sulfonate) (PEDOT:PSS)	• Ink showed remarkable printability. • Printed samples were found to be wet stable and showed excellent electrochemical and electrical performance, that is, a conductivity of 30 S/cm, tensile strains (>40%), and specific capacitances of 211 F/g • PEDOT:PSS accounts for only 40 wt% of the total ink composition.	[123]
Electronic devices	Electrochemical energy storage devices	CNFs with different surface chemistries were utilized to enhance the rheology of MXenes based inks	• After the addition of CNFs, resultant inks showed exceptional 3D printability. • Different 3D architectures with excellent geometric and shape accuracy were printed utilizing the optimized ink, at a low solid content, generating progressivity porous structures after being freeze-dried. • A 3D super capacitor developed from a hybrid link showed an areal capacitance, energy density and power density of 2.02 F cm^{-2}, 101 μ Wh cm^{-2} and 0.299 mW cm^{-2}, respectively. Further, it also maintains an 85% capacitance retention rate after 5000 cycle	[125]
Electronic industry	Designing materials for IR stealth and EMI shielding	CNFs, having high aspect ratio were utilized as a fortifying and a rheological modifier agents for MXene/CNF colloids	• MXene/CNF film displayed a remarkably increased electrical conductivity (46 685 S m^{-1}), tensile strength (281.7 MPa), and Young's modulus (14.8 GPa). • IR stealth and EMI shielding effectiveness was found to be 0.562 emissivity and 50.2 dB, respectively. • To define the optimal solution-processing	[124]

(Continues)

TABLE 3 (Continued)

Field of application	Application	Treatment applied onto NC	Remarks/conclusion	References
			parameters systematical rheological study of the MXene/CNF colloids is done.	
Colloidal stabilization	To stabilize simultaneously both TiO_2 nanoparticles and oil droplets in the same colloidal solution	Both anionic and cationic CNFs were used.	• The obtained suspensions, regardless of surface charge and pH, retained their stability for up to 2 months. • A complex network generation between nanofibers and TiO_2 particles was reported and is found to be responsible for the stabilization of inorganic particles and oil droplets.	[140]
Oil and gas industry	Modifiers for fracturing fluids	Lignin containing CNFs (13.7% lignin)	• The CNFs suspensions displayed gel-like viscoelastic characteristics and typical shear-thinning behaviors. • Lignin-containing CNFs significantly enhanced yield stress, zero-shear viscosity, thermal quality as well as the shear-thinning ability of Gaur gum-based viscoelastic fracturing fluids. • The resultant suspension exhibited excellent proppant-suspending ability and is confirmed by uniform dispersion of sand particles in the fluids without settling even after standing for different temperatures (80 and 25°C) for 24 h.	[141]
Oil Industry	Improve the rheology of WDFs in oil industry	BT was used along with untreated CNFs as a viscosity and filtration-improving agent	• Synthesized CNF suspensions exhibited shear thinning behavior and solid-like viscoelastic characteristics due to highly entangled networks • Even a small amount of CNF (0.5 wt%) was able to substitute half of BT in WDFs, and resulted in fluids showed good rheological and filtration properties.	[131]

TABLE 3 (Continued)

Field of application	Application	Treatment applied onto NC	Remarks/conclusion	References
			• WDFs/CNFs showed remarkable shear-thinning behaviors at high shear rates • The viscosity of WDFs increased (0.05 to 102.7 Pa s at the lowest shear rate 0.1 s-1) with an increase (0 to 1 wt%) in the % CNFs contents	
Food industry	Fat reducer in Food industry	Un-treated CNFs	• Different concentrations of CNFs were used to formulate reduced fat 5%, 15%, and 30% mayonnaise. • CNF acts as an ideal candidate to act as a fat mimetic and emulsion stabilizer in the food system. • G′ value for samples after incorporation of CNFs was found to be higher than G″, indicating elastic characteristics for mayonnaise samples. • At higher fat reduction (30%), an increased amount of water is added, which will cause a reduction in the viscosity of mayonnaise, and thus, to mitigate the loss of rheological characteristics, an increased amount of CNF (0.3%) was added.	[126]
Food industry	As milk thickener in the Food industry	CNFs extracted from brown algae	• Milk was greatly thickened when CNFs were added to it because of the CNFs's casein micelles' absorbing ability through hydrogen bonding. • Cell viability was observed to be 100% across all samples and was hardly impacted by CNF dosage.	[127]
Polymer industry	Improve low melt strength and slow crystallization rate of Polylactic acid	Acetylated CNFs were dispersed in polylactic acid using melt-compounding technique	• Melt elasticity and crystallization properties of PLA were significantly enhanced.	[120]

(Continues)

TABLE 3 (Continued)

Field of application	Application	Treatment applied onto NC	Remarks/conclusion	References
			• Foaming behavior improved after lading of 2 wt.% acetylated CNFs. • Prepared nanocomposite foams showed a maximum of 20.4 expansion ratio.	
Polymer industry	Improve the rheology of Polyvinyl alcohol (PVA)	TEMPO-oxidized CNFs	• Steady and dynamic rheology indicated that suspension is pseudoplastic and shows thixotropic and/or shear thinning behavior. • In the dilute regime, PVA suspension exhibited gel-like characteristics and changes to a liquid-like state with an increase in frequency. • The resulting suspension showed liquid-like behavior at semi dilute the PVA concentration.	[121]
Polymer industry	To modify the rheological characteristics of polyol commonly used in polymer, food, and paint industries as compatibilizer, precursor and viscosity controller		• The steady-shear rheological tests revealed four distinct flow behavior regimes correlated to rising yield stress and viscosity with increased CNF loading in the polyol. • Employing oscillatory-shear rheology, the critical concentration of CNF for the creation of a percolation system has been identified.	[118]
Automobile, aerospace, industry, bio-medical, etc.	As rheological Modifiers in Magnetorheological Fluids, which can be subsequently used in mechanical systems, oil &gas drilling, biomedicine, and electronic controls	Untreated CNF	• CNFs improve the suspension of magnetic particles in CNF-Magnetorheological Fluid, thus further enhancing the stability and magnetorheological characteristics (cycling results in viscosity stability, with a reversible rate of 95.57% after 100 cycles). • Due to a magnetic dipole–dipole interaction, magnetic nanoparticles are aligned in the direction of the used magnetic field, improving the rheology.	[122]

TABLE 3 (Continued)

Field of application	Application	Treatment applied onto NC	Remarks/conclusion	References
Automobile, aerospace, industry, bio-medical, etc.	Additives for aqueous carbonyl iron particles (CIPs) based magnetorheological (MR) fluids	Untreated CNFs	• CNFs with higher aspect ratios effectively prevented CIP chains from coalescing into stronger columns as compared to CNCs, producing MR fluids with standard thixotropic behavior. • The percolated CNFs network, which functions as a stress enhancer, is not present in the case of CNCs, and was found to be responsible for the increased magneto-responsive levels at a comparable 0.3 wt% CNFs concentration. • Since the percolated CNF network functions as a stress multiplier, the presence of CNF even increases the magneto-responsive levels at the comparable concentration (0.3 wt%).	[142]
Automobile, aerospace, industry, bio-medical, etc.	For stabilization of magnetic particles (MPs) inmagnetorheological fluids (MFs)	Lignin containing CNFs	• CNFs enhanced the suspension of MPs in MFs, which in turn increased the yield stress, viscosity and dynamic moduli of MFs over the entire range of magnetic field (0–1 T). • CNFs-MFs showed excellent magnetorheological characteristics, that is, good reversibility, quick magnetic response and outstanding cycling strength.	[143]
Bio-medical applications	Bio-ink preparation	Pluronic and Alginate hydrogels were blended with CNFs and polycaprolactone microfber	• An extrusion-based bio-printer utilized to extrude the fabricated composites for strut spreading experiments. • The cartridges were heated for 20 min at 25°C prior to printing, and printing was done with high-precision 21G-12.7 mm blunt needles.	[144]

(Continues)

TABLE 3 (Continued)

Field of application	Application	Treatment applied onto NC	Remarks/conclusion	References
			• CNFs improved the shape fidelity of hydrogels, whereas polycaprolactone enhanced the viscosity bio-ink but caused loss of structural integrity with time in Pluronic • Increased complex viscosity with increasing filler concentration was noted. • CNFs showed significant rheological impact even at very low concentrations (0.5–2% w/v), whereas a higher amount of PCL microfibers are required (5%–10% w/v) to have equivalent effects.	
Bio-medical applications	Tissue engineering or cartilage regeneration	Untreated, carboxylated and commercial CNFs were used for the preparation of cold extrusion waterborne, polyurethane-urea (WBPU)/CNFs3Ddirect ink writing purpose	• CNFs modulated the rheology of WBPU dispersion, and the prepared ink's rheology was seen to be largely dependent on the CNF contents. • Ex situ method of preparing inks displayed higher gel-like characteristics than in situ method because of better water/CNFs interactions. • Carboxylated CNFs showed improved interactions than pristine CNF, resulting in better-fortified materials • All prepared inks displayed non-Newtonian shear-thinning characteristics, which is particularly ideal for direct ink writing	[132]
Bio-medical applications	Developing bio-ink for tissue engineering and bio-medical applications	TO-CNFS utilized	• To improve the bio-ink quality, pectin, in combination with CNFs, was used. • Relative amounts of CNFs and Pectin varied and optimized in terms of rheological characteristics, and optimized concentration	[133]

TABLE 3 (Continued)

Field of application	Application	Treatment applied onto NC	Remarks/conclusion	References
			was 1 and 2.5% w/v, respectively. • The addition of TO-CNFs increases the inks' viscosity while maintaining shear thinning response • The maximum printing accuracy was found to be 93% ± 1%, 93% ±4%, and 86% ± 10% for 3D printing nozzle having diameters 22, 20, and 18 G, respectively, when printing was done at a writing speed of 24 mm/s. • L929 fibroblast cells were used to create bio-inks, which were discovered to be stable in physicochemically similar conditions.	
Bio-medical fields	in vivo survival and neovascularization of the 3D bio-printed grafts	CNFs mixed with alginate in a ratio 4:1 was used	• Extrusion 3D bio-printer with a nozzle size of 800 μm at a printing pressure of 3 kPa was used • The 3D-bioprinted constructions of lipoaspirate-derived adipose tissue (LDAT) retained their structural integrity and cellular makeup. • LDAT demonstrated good printability, sustained 3D bio-printing and tissue regeneration in vivo, and showed signs of vascularization on both a microscopic and macroscopic scale. • $CaCl_2$ was used as a crosslinker during post-printing. • Bio-compatibility was performed with stromal/stem cells generated from adipose tissue.	[134]
Bio-medical field	For Neural-cell Culturing and generation of vitro 3D neural model to study the cause and mechanism for neurodegenerative illness	CNFs, along with single-wall carbon nanotubes (SWCNT) and Alginate taken in different ratio 70:10:20) and (60:20:20	• Inkredible + bioplotter bioprinter at a pressure of 15 kPa was used. • CNFs/CNT-based conductive inks are used in the 3D printing of	[135]

(Continues)

TABLE 3 (Continued)

Field of application	Application	Treatment applied onto NC	Remarks/conclusion	References
			brain cell differentiation scaffolds. • The conductive characteristics of CNTs (at 10 wt%) facilitated communication among distant brain cells. • By calcium-induced cross-linking of alginate, 3D printed scaffolds' electrical conductivity has been adjusted. • Bio-compatibility was confirmed against human neuroblastoma cells (SH-SY5Ycell line)	
Bio-medical field	Bio-ink rheology improved for bone tissue engineering	TO-CNFs	• Bio-ink was developed by using CNFs, alginate and polydopamine nanoparticles • Extrusion-based 3D printing technique was employed. • An increase in ink viscosity, recovery rate and mechanical strength was observed. • All samples showed shear thinning behavior. • Metabolic activities were enhanced • improved osteogenesis-related expression of the gene was seen.	[136]
Drug delivery	Bioink composed of alginate (4 wt.%) and CNF (1–5 wt.%)were developed for curcumin administration (loaded at 15 wt.%)	Untreated CNFs	• CNF successfully reinforced the scaffolds and modulated their porosity. • Curcumin-filled bioinks were successfully 3D printed and after in vitro release tests, it has been found that its stability depends upon both alginate and CNF amount. • Curcumin release kinetics found to depend on both amount of CNF and scaffold disintegration. • CNF amounts <3 wt.% did not demonstrate the necessary characteristics to provide shape integrity after printing.	[137]

TABLE 3 (Continued)

Field of application	Application	Treatment applied onto NC	Remarks/conclusion	References
Bio-medical applications	Self-healing CNFs-fortified alginate hydrogel for bone repairing	CNFs-fortified oxidized alginate/gelatin semi-interpenetrating network hydrogel using the combined impacts of hydrogen bonds and dynamic imine was developed.	• The hydrogel showed alluring injectability with a gelation time (of ∼150 s). • Self-healing efficiency was found to be 92%, which may result in minimally invasive, dynamic adjustments and personalized therapies. • Also, synthesized gel showed enhanced (96%) preosteoblast cell (MC3T3-E1) viability, osteogenic differentiation and proliferation.	[145]

HPH was increased.[110] Pressure and time of passes of HPH play a very significant role in fibrillation and ultimately in G′ of suspensions. For example, for enzymatically produced CNFs, storage modulus was found to increase with the increase in HPH pressure from 500 to 1000 bars[111]; contrary to this, in another study, maximum G′ for untreated CNFs was found only after the 2 passes through HPH, and was noticed to decrease with a further increase in a number of passes.[112] Such variations in G′ have been attributed to an increase in the degree of fibrillation with additional HPH passes. Thus, there is a strong need to characterize the CNF surface characteristics across different length scales. Since the rheological characteristics of CNF suspension depend on both the length and diameter of CNFs, whose measurement is quite tedious as CNFs are generally long and highly flexible.

4.2.3 | Rheology variation with the type of surface functionalization/extraction technique employed

Lee et al.[113] studied the impact of both amounts of carboxyl content and time for HPH on the viscosity and G′ of the prepared CNFs. It has been reported that the time of HPH as well as surface charge or carboxyl contents, impact the length or aspect ratio of synthesized CNFs and, ultimately, their rheology properties. The greater the charge on fibers surface, the ease with which nanofibers can be obtained, and the higher charge will also lead to better-sized CNFs. Further increase in the timing of HPH and the surface charge has led to an increase in viscosity and G′ of CNFs suspension. Similarly, the impact of various surface modification techniques such as TO-CNF,[113,114] carboxymethylation[115](Figure 6) and periodate–chlorite oxidation (PC-CNF)[116] on carboxyl contents of synthesized CNFs and ultimately rheology properties of CNFs suspension was also examined. It has been observed for all samples that viscosity, G′ or yield stress increase with increases in carboxyl contents. However, after reaching their maximum for some samples, the viscosity decreases with further increases in carboxyl contents due to better dispersion and low aspect ratio of CNFs suspensions.

5 | ADVANCED APPLICATIONS OF NANO CELLULOSE AS RHEOLOGY MODIFIERS

Compared to existing literatures,[35,36] here the recent efforts made to control the rheology of NC suspension in multiple fluids by blending it with some other bio-additives or by employing surface modification/extraction, techniques have been reviewed. Tables 3 and 4 illustrate the work done in the last 2–3 years and clearly highlight the value of NC's distinctive rheological qualities for a wide range of applications.[84,120–149] Some of the top-notch characteristics that specifically define the distinctive rheological features of NC suspensions and their ability to act as rheology modifiers in diverse applications include their large water retention/holding potential, remarkable shear thinning behavior, their capabilities to align at high shear rates, thickening impact, and their capacity to form thixotropic frameworks that excellent restoration phenomena. The literature review

TABLE 4 Potential of CNCs as rheology modifiers in multiple fields.

Field of application	Application	Treatment applied onto NC/type of CNCs	Remarks/conclusion	References
Oil industry	Modify the rheology of perfluoropolyether oil	The living radical polymerization technique was applied for bonding of fluoropolymer onto CNCs surface	• Perfluoropolyether-based hybrid oils thickened remarkably upon the addition of functionalized CNCs. • The addition of CNCs raises viscosity, enhances thixotropy efficiency, and improves G′ and G″. • The change of G′ > G″ from the flowable to the grease-like state in hybrid oils has been confirmed upon adding 10–15 wt% functionalized CNCs. • Such behavior has been associated with the development of a stable network between grafted CNCs and PFPE oil.	[84]
Food industry	To improve rheology of DIW based 3D printing of a variety of foodstuffs including tomato puree, spinach puree, and applesauce.	Freeze dried CNCs	• The presence of a higher amount of water (more than 88%) in the food bases gave ample capability for CNCs to design a shear-thinning gel matrix within the dense food granules. • CNCs enhanced shear-thinning behavior in the feedstocks, which is necessary for better flow of bio-ink through the nozzle during printing.	[128]
Bone and tissue engineering	To improve the fixation time of each printing layer by using combined approach of photoinitiator as polymerization causing agent and CNCs as rheology controller	Untreated CNCs	• HaakeRheostress 6000 rheometer, made up of Thermo Fisher Scientific, was used at 20°C temperature. • After being strengthened with CNC, acrylic acid/ Poly(ethylene glycol) diacrylate (PEGD), based hydrogels were 3D printed and photopolymerized using a water-compatible photoinitiator system [2,4,6-trimethylbenzoyl-diphenylphosphine oxide (5 wt.%) and poly(ethylene glycol) hexadecyl ether (Brij 58) (95%)]. • Shear-thinning behavior was noted and Viscosity	[138]

TABLE 4 (Continued)

Field of application	Application	Treatment applied onto NC/type of CNCs	Remarks/conclusion	References
			increased with the rise in CNC concentrations, although shear thinning behavior was preserved at high concentrations. • Bio-inks containing CNCs showed thixotropic characteristics. • Samples with a higher CNC content took longer to sustain their viscosity. When the ink contains 2.4% CNCs, a maximum recovery of 70.36% was attained in 15 s. • Rapid photopolymerization (6.25 s/mm) of acrylic acid and PEGD, at very low concentration (0.8–0.9 g) of photoinitiator, after printing and curing of each layer by 405 nm light assisted in overcoming the typical height limit of DIW printing of hydrogels and enabled the development of materials with a better aspect ratio.	
Feed lines of transporting slurry	To improve the rheology of magnesium oxide/lime slurries and to reduce scale formation	Untreated CNCs and anionic/cationic and non-ionic/vinyl monomers grafted CNCs used as rheology modifying agents	• In addition to their ability to adjust rheology, modifiers help lessen or prevent the buildup of scale inside transfer pipes that is brought on by the solids settling out of the slurry and solidifying.	[146]
Concrete industry	To modify the rheology of cement pastes	S-CNCs, controlled acid hydrolysed and transition metal oxidized CNCs were used as rheology modifier	• Neither the size, type of extraction techniques employed and zeta potential values of CNCs showed a significant impact on the rheological characteristics of cement pastes. • The potential of CNC as viscosity modifying ingredients was noted at concentrations (>0.5%), whereas at <0.2%, it works as water reducing agent.	[119]
Water industry	Role of CNCs as rheology modifier or to enhance the	S-CNCs were used as a modifier	• CNCs improve the dope dispersions' viscoelastic	[147]

(Continues)

TABLE 4 (Continued)

Field of application	Application	Treatment applied onto NC/type of CNCs	Remarks/conclusion	References
	water permeability of polyethersulfone membranes		properties, resulting in a slower exchange of nonsolvent/solvent during the phase separation. • The viscosity of the mixture increased with an increase in CNCs concentration. • The prolonged time needed to develop finger-like openings toward the membrane bottom during the nonsolvent-induced phase separation is caused by the increased viscosity of dope dispersion.	
Bio-medical	To improve the rheology of oxidized dextran/gelatin based bioink for tissue engineering	0.04% S-CNCs were mixed with 2% oxidized dextran/2% gelatin to develop bio-ink	• Oxidized dextrin showed a remarkable impact on the printability of the hydrogels. • Scaffold porosity was noticed to be improved after the addition of CNCs • Bioprinter named Bio-Architect (Regenovo Biotechnology Co. Ltd.) at 48 kPa pressure, 20 mm/s printing speed and 220 μm nozzle size were used. • Bio-compatibility was studied against 3 T3 cells.	[148]
Food and cosmetics industry	Improve rheology of oil in water Pickering emulsion	Carboxylated CNCs (cCNCs)	• Sodium periodate/Fenton was utilized to create needle-like cCNCs, which were subsequently used as an emulsifier to create oil in water Pickering emulsion. • SF-cCNC interfacial adsorption, rather than the development of a spatial network between droplets, was acknowledged for stabilizing the emulsion • Pickering emulsion's outstanding anti-agglomeration qualities and long-term stability may explore their remarkable potential to develop cosmetic and food goods.	[129]

TABLE 4 (Continued)

Field of application	Application	Treatment applied onto NC/type of CNCs	Remarks/conclusion	References
Food, pharmaceuticals and cosmetics industry	Formulation of sustainable plant-based multiphase systems for food, cosmetics, and pharmaceuticals.	S-CNCs	• S-CNCs and partially deacetylated nano chitin-based suspension, [with different relative proportions of CNCs (0.25 wt.%) and nano chitin(0–0.25 wt.%)] was utilized as water phase and sunflower oil (10–50 wt.%) as oil phase to develop Pickering emulsion. • When the S-CNCs/nano chitin mass ratio was less than 1.25, the resulting emulsions exhibited long-term storage ability at ambient conditions. • Different oil concentrations in the emulsions showed elastic behavior and resilience toward coalescence. • The higher loading of chitin promoted the formation of physical networks; however, upon an increase in oil amounts, an increase in inter-droplet interactions was observed.	[130]
Cosmetics, paper, food industry, etc.	CNCs role in improvement in rheology of gelling agents coating slurries, etc.	S-CNCs	• S-CNCs hydrogels displayed two flow regimes, that is, a quasilinear regime followed by the stress hardening stage for CNC hydrogel. • Although flow stress evolved non-linearly, the compression modulus increased as the strain rate increased.	[117]
Bio-medical field	Improve the rheology of bio-ink for meniscal tissue bio-printing	Carboxylated CNCs	• BIO X bioprinter (Cellink) with 25 G needles diameter at pressure < 55 kPa gives the best result. Its printed and printhead temperatures weremaintained at 10 and 25°C, respectively. • The constructs were crosslinked with sterile	[149]

(Continues)

TABLE 4 (Continued)

Field of application	Application	Treatment applied onto NC/type of CNCs	Remarks/conclusion	References
			200 mM calcium chloride ($CaCl_2$) • All bio-ink exhibited shear thinning behavior and solid-like behavior till the G′/G″ cross over • Bio-ink was developed by using different relative proportions of carboxylated-CNCs, alginate and gelatin • After the rheology study, the optimum amount of gelatin, alginate and CNCs components of bioink was found to be 4.0%, 0.75%, and 1.4%, respectively. • It was discovered that the synthetic bioink was bio-compatible, printable, increase the osteogenic markers genes expression, increase the viability in cell culture (> 98% cell viability), and preserve the chondrocytes' natural phenotype.	
Biomedical applications	Improve rheology of bio-ink for 3D bio-printing of scaffolds for bone tissue designing	S-CNCs	• CNCs (0–2 wt.%)/chitosan (2 wt.%)/hydroxyethyl cellulose (0.1–0.5 mg/mL)/glycerophosphate-based bio-ink was developed. • Bio-printing was done using an extrusion-based 3D technique, and MC3T3-E1 cells (a pre-osteoblast cell line) were utilized for the formation and bio-compatible of bio-ink. • An increased in ink viscosity and mechanical toughness was noted. • Higher expression of osteogenic markers • An increase in mineral deposition and alkaline phosphate activity was noted. • Bio-compatible bio-ink assisted the cell encapsulation at 5 million cells/mL cell density.	[139]

carried out in the present section makes clear the emerging and cutting-edge applications of NCs as rheology modulators in the coating[117] and paint industries[118] as well as a rheology modulator for cement,[119] composites,[118,120–122] electronic devices,[122–125] cosmetics, foods,[117,126–130] drilling fluids,[122,131] and so forth. The superior mechanical, shear thinning, and bio-compatible/non-cytotoxic qualities of NC have also piqued researchers' attention in developing 3D bio-printing materials for creating viable living human organs/tissues.[125,128,132–139] From the tables, it can be concluded that both CNFs and CNCs have remarkable potential as rheology modifiers/modulators in multiple fields; however, the rapid expansion of such applications at the industrial level is constrained by issues related to their complicated structure and the consistency of production in regards to various features of NC that dramatically influence their rheological behavior.

6 | CONCLUSION

From the above discussion, it is clear that NCs have remarkable potential in controlling the rheology of different fluids. Their unique properties, such as highly tunable viscosity, considerable shear thinning behavior, thixotropic qualities, and remarkable emulsion stabilization capabilities, have been found to vary strongly with the dimensions/aspect ratio and types of surface functionalization/extraction technique employed. Rheological properties of functionalized CNCs and CNFs additives were found to depend upon the lyotropic phase of CNCs and flocculation of CNF and their shear-induced alignment. Between CNCs and CNFs, the former, due to low dimensions/aspect ratio, have been found to align themselves more readily along shear rate. Further, CNCs with larger aspect ratios showed almost the same rheological behavior as that of CNFs at higher concentration; however, at low concentrations a transformation from solid to fluid-like behavior was observed. NC with a higher aspect ratio resulted in more complex steady state-flow behavior and showed solid-like viscoelastic characteristics. Further, the method of surface functionalization employed has a substantial impact on the charge density and hydrophilic nature of NC, which in turn controls the interparticle attraction/repulsion and thus affects the overall characteristics of NC suspension.

The CNCs and CNFs as additives have been widely utilized to control the rheology of different fields, such as for the formation of bio-ink for printing 3D electronic, biomedical and other devices; fluids in oil recovery and drilling gas/oil wells; gelling and thickening agents in the food industry, as well as for the formation of cosmetic products; and viscosity controllers in the concrete industry. It is more crucial to employ suitable surface functionalization or NC extraction technique and characterize the synthesized NC comprehensively before employing it for a particular application. Further, acetylated, lignin modified, carboxylated, fluoropolymer grafted or after blending with PEDOT:PSS, NC additives showed huge potential in controlling the mechanical strength and viscoelastic properties of bio-inks, gels, oils, transporting slurry and other fluids in comparison to untreated NC.

Aside from the fascinating characteristics of NC as a rheological modifier additive, certain factors limit its large-scale applications. Some of their limitations are their complex structure; issues related to the production process's reproductivity; higher cost of production, surface functionalization, storage and transport; variability in their dimensions, composition and surface characteristics. Thus, special attention is needed from researchers worldwide to resolve these issues and fully explore their potential as rheology modifiers. Further, researchers should also focus on the development of new NC/nanomaterials testing standards for effective utilization of NC fillers, develop new functionalization techniques and test new hydrophilic/hydrophobic polymers to boost the NC suspension's processability. The bio-polymers such as chitin, chitosan, lignin, and so forth, may be blended with NC additives to form infinite tunable systems to improve the rheology of numerous fluids and thus fulfill growing demands of NC based rheology modifiers in multiple fields.

AUTHOR CONTRIBUTIONS

It is confirmed that both authors (Ashvinder K. Rana and Vijay K. Thakur) have equally made a substantial contribution to the concept or design, daft or revise and aprrove the final version of review article to be published.

DATA AVAILABILITY STATEMENT

The data that support the findings of this study are available from the corresponding author upon reasonable request.

ORCID

Vijay Kumar Thakur https://orcid.org/0000-0002-0790-2264

REFERENCES

[1] C. Calvino, N. Macke, R. Kato, S. J. Rowan, *Prog. Polym. Sci.* **2020**, *103*, 101221.
[2] A. S. Singha, A. K. Rana, *J. Reinf. Plast. Compos.* **2012**, *31*, 1538.
[3] B. Ates, S. Koytepe, A. Ulu, C. Gurses, V. K. Thakur, *Chem. Rev.* **2020**, *120*, 9304.

[4] V. K. Thakur, S. I. Voicu, *Carbohydr. Polym.* **2016**, *146*, 148.
[5] M. K. Thakur, A. K. Rana, V. K. Thakur. Lignocellul. Polym. Compos. Process. Charact. Prop. Vol 9781118773574 Wiley Blackwell 2014, 1.
[6] A. K. Rana, F. Scarpa, V. K. Thakur, *Ind. Crop. Prod.* **2022**, *187*, 115356.
[7] B. Thomas, M. C. Raj, J. Joy, A. Moores, G. L. Drisko, C. Sanchez, *Chem. Rev.* **2018**, *118*, 11575.
[8] D. Klemm, F. Kramer, S. Moritz, T. Lindström, M. Ankerfors, D. Gray, A. Dorris, *Angew. Chem. Int. Ed.* **2011**, *50*, 5438.
[9] A. K. Rana, E. Mostafavi, W. F. Alsanie, S. S. Siwal, V. K. Thakur, *Ind. Crop. Prod.* **2023**, *194*, 116331.
[10] A. Pappu, K. L. Pickering, V. K. Thakur, *Ind. Crop. Prod.* **2019**, *137*, 260.
[11] S. Beluns, S. Gaidukovs, O. Platnieks, G. Gaidukova, I. Mierina, L. Grase, O. Starkova, P. Brazdausks, V. K. Thakur, *Ind. Crop. Prod.* **2021**, *170*, 113780.
[12] A. S. Singha, A. K. Rana, *Int. J. Polym. Anal. Charact.* **2012**, *17*, 72.
[13] A. K. Rana, E. Frollini, V. K. Thakur, *Int. J. Biol. Macromol.* **2021**, *182*, 1554.
[14] A. K. Rana, V. K. Thakur, *Mater. Adv.* **2021**, *2*, 4945.
[15] D. Zielińska, T. Rydzkowski, V. K. Thakur, S. Borysiak, *Ind. Crop. Prod.* **2021**, *161*, 113188.
[16] O. Platnieks, A. Sereda, S. Gaidukovs, V. K. Thakur, A. Barkane, G. Gaidukova, I. Filipova, A. Ogurcovs, V. Fridrihsone, *Ind. Crop. Prod.* **2021**, *169*, 113669.
[17] N. Uppal, A. Pappu, V. K. S. Gowri, V. K. Thakur, *Ind. Crop. Prod.* **2022**, *182*, 114895.
[18] R. J. Moon, A. Martini, J. Nairn, J. Simonsen, J. Youngblood, *Chem. Soc. Rev.* **2011**, *40*, 3941.
[19] A. K. Rana, Y. K. Mishra, V. K. Gupta, V. K. Thakur, *Sci. Total Environ.* **2021**, *797*, 149129.
[20] A. Dufresne, *Mater. Today* **2013**, *16*, 220.
[21] A. K. Rana, *Curr. Opin. Green Sustain. Chem.* **2022**, *38*, 100696.
[22] A. K. Rana, V. K. Gupta, A. K. Saini, S. I. Voicu, M. H. Abdellattifaand, V. K. Thakur, *Desalination* **2021**, *520*, 115359.
[23] R. Reshmy, E. Philip, A. Madhavan, A. Pugazhendhi, R. Sindhu, R. Sirohi, M. K. Awasthi, A. Pandey, P. Binod, *J. Hazard. Mater.* **2022**, *424*, 127516.
[24] M. F. Ismail, A. H. Jasni, D. J. Ooi, *Polym. Polym. Compos.* **2021**, *29*, 814.
[25] M. E. Lamm, K. Li, D. Ker, X. Zhao, H. E. Hinton, K. Copenhaver, H. Tekinalp, S. Ozcan, *Cellulose* **2022**, *29*, 3859.
[26] A. B. Perumal, R. B. Nambiar, J. A. Moses, C. Anandharamakrishnan, *Food Hydrocoll.* **2022**, *127*, 107484.
[27] F. A. Silva, F. Dourado, M. Gama, F. Poças, *Nanomaterials* **2020**, *10*, 2041.
[28] B.-M. Tofanica, D. Belosinschi, I. Volf, *Gels* **2022**, *8*, 497.
[29] M. Kaushik, A. Moores, *Green Chem.* **2016**, *18*, 622.
[30] A. A. Septevani, D. Burhani, Y. Sampora, *Nanocellulose Materials*, Elsevier, Netherlands **2022**, p. 217.
[31] J. P. Lagerwall, C. Schütz, M. Salajkova, J. Noh, J. Hyun Park, G. Scalia, L. Bergström, *NPG Asia Mater.* **2014**, *6*, e80.
[32] M. Kim, S. Kim, N. Han, S. Lee, H. Kim, *Carbohydr. Polym.* **2023**, *300*, 120218.
[33] S. O. Ilyin, S. N. Gorbacheva, A. Y. Yadykova, *Tribol. Int.* **2023**, *178*, 108080.
[34] H. Ma, J. Zhao, Y. Liu, L. Liu, J. Yu, Y. Fan, *Ind. Crop. Prod.* **2023**, *192*, 116081.
[35] C. Yadav, A. Saini, W. Zhang, X. You, I. Chauhan, P. Mohanty, X. Li, *Int. J. Biol. Macromol.* **2021**, *166*, 1586.
[36] M.-C. Li, Q. Wu, R. J. Moon, M. A. Hubbe, M. J. Bortner, *Adv. Mater.* **2021**, *33*, 2006052.
[37] D. Beyene, M. Chae, J. Dai, C. Danumah, F. Tosto, A. Demesa, D. Bressler, *Materials* **2018**, *11*, 1272.
[38] T. Nissilä, J. Wei, S. Geng, A. Teleman, K. Oksman, *Nanomaterials* **2021**, *11*, 490.
[39] M. Le Gars, L. Douard, N. Belgacem, J. Bras, in *Smart Nanosystems for Biomedicine, Optoelectronics and Catalysis* (Eds: T. Shabatina, V. Bochenkov), IntechOpen, London, UK **2020**.
[40] A. K. Rana, S. Guleria, V. K. Gupta, V. K. Thakur, *Bioresour. Technol.* **2022**, *367*, 128255.
[41] E. Hafemann, R. Battisti, D. Bresolin, C. Marangoni, R. A. F. Machado, *Waste Biomass Valoriz.* **2020**, *11*, 6595.
[42] V. Nang An, C. Nhan, H. Thuc, T. D. Tap, T. T. T. Van, P. Van Viet, L. Van Hieu, *J. Polym. Environ.* **2020**, *28*, 1465.
[43] C. J. Wijaya, S. Ismadji, H. W. Aparamarta, S. Gunawan, *ACS Omega* **2020**, *5*, 20967.
[44] O. M. Vanderfleet, D. A. Osorio, E. D. Cranston, *Philos. Trans. R Soc. Math. Phys. Eng. Sci.* **2018**, *376*, 20170041.
[45] X. Sang, C. Qin, Z. Tong, S. Kong, Z. Jia, G. Wan, X. Liu, *Cellulose* **2017**, *24*, 2415.
[46] Y. Habibi, H. Chanzy, M. R. Vignon, *Cellulose* **2006**, *13*, 679.
[47] T. Saito, S. Kimura, Y. Nishiyama, A. Isogai, *Biomacromolecules* **2007**, *8*, 2485.
[48] O. Nechyporchuk, M. N. Belgacem, J. Bras, *Ind. Crop. Prod.* **2016**, *93*, 2.
[49] L. Lin, S. Jiang, J. Yang, J. Qiu, X. Jiao, X. Yue, X. Ke, G. Yang, L. Zhang, *Int. J. Bioprint.* **2022**, *9*, 212.
[50] K. Hyun, M. Wilhelm, C. O. Klein, K. S. Cho, J. G. Nam, K. H. Ahn, S. J. Lee, R. H. Ewoldt, G. H. McKinley, *Prog. Polym. Sci.* **2011**, *36*, 1697.
[51] R. Kádár, S. Spirk, T. Nypelö, *ACS Nano* **2021**, *15*, 7931.
[52] S. Beck-Candanedo, M. Roman, D. G. Gray, *Biomacromolecules* **2005**, *6*, 1048.
[53] E. E. Ureña-Benavides, G. Ao, V. A. Davis, C. L. Kitchens, *Macromolecules* **2011**, *44*, 8990.
[54] X. M. Dong, T. Kimura, J.-F. Revol, D. G. Gray, *Langmuir* **1996**, *12*, 2076.
[55] M. Bercea, P. Navard, *Macromolecules* **2000**, *33*, 6011.
[56] H.-N. Xu, Y.-Y. Tang, X.-K. Ouyang, *Langmuir* **2017**, *33*, 235.
[57] W. J. Orts, L. Godbout, R. H. Marchessault, J.-F. Revol, *Macromolecules* **1998**, *31*, 5717.
[58] T. Ebeling, M. Paillet, R. Borsali, O. Diat, A. Dufresne, J.-Y. Cavaillé, H. Chanzy, *Langmuir* **1999**, *15*, 6123.
[59] N. Yoshiharu, K. Shigenori, W. Masahisa, O. Takeshi, *Macromolecules* **1997**, *30*, 6395.
[60] S. Shafiei-Sabet, W. Y. Hamad, S. G. Hatzikiriakos, *Langmuir* **2012**, *28*, 17124.
[61] Y. Xu, A. D. Atrens, J. R. Stokes, *J. Colloid Interface Sci.* **2017**, *496*, 130.
[62] D. Liu, X. Chen, Y. Yue, M. Chen, Q. Wu, *Carbohydr. Polym.* **2011**, *84*, 316.

[63] A. Mohd Shahabuddin, H. Alhuribi, K. N. Mohd Amin, *Mater. Today Proc.* **2022**, *57*, 1356.
[64] H. Oguzlu, C. Danumah, Y. Boluk, *Curr. Opin. Colloid Interface Sci.* **2017**, *29*, 46.
[65] Y. Tang, X. Wang, B. Huang, Z. Wang, N. Zhang, *Polymer* **2018**, *10*, 278.
[66] B. Peng, J. Tang, P. Wang, J. Luo, P. Xiao, Y. Lin, K. C. Tam, *Cellulose* **2018**, *25*, 3229.
[67] M.-C. Li, Q. Wu, K. Song, S. Lee, Y. Qing, Y. Wu, *ACS Sustain. Chem. Eng.* **2015**, *3*, 821.
[68] S. Shafiei-Sabet, W. Y. Hamad, S. G. Hatzikiriakos, *Cellulose* **2014**, *21*, 3347.
[69] L. Zhou, H. He, M.-C. Li, K. Song, H. N. Cheng, Q. Wu, *Carbohydr. Polym.* **2016**, *153*, 445.
[70] T. Moberg, K. Sahlin, K. Yao, S. Geng, G. Westman, Q. Zhou, K. Oksman, M. Rigdahl, *Cellulose* **2017**, *24*, 2499.
[71] L. Du, T. Zhong, M. P. Wolcott, Y. Zhang, C. Qi, B. Zhao, J. Wang, Z. Yu, *Cellulose* **2018**, *25*, 2435.
[72] Q. Wu, Y. Meng, S. Wang, Y. Li, S. Fu, L. Ma, D. Harper, *J. Appl. Polym. Sci.* **2014**, *131*, 40525.
[73] A. Babaei-Ghazvini, B. Acharya, *Carbohydr. Polym. Technol. Appl.* **2022**, *3*, 100217.
[74] M. A. Hubbe, P. Tayeb, M. Joyce, P. Tyagi, M. Kehoe, K. Dimic-Misic, L. Pal, *Bioresources* **2017**, *12*, 9556.
[75] A. Lu, Y. Wang, Y. Boluk, *Carbohydr. Polym.* **2014**, *105*, 214.
[76] A. Naderi, T. Lindström, T. Pettersson, *Cellulose* **2014**, *21*, 2357.
[77] T. Abitbol, D. Kam, Y. Levi-Kalisman, D. G. Gray, O. Shoseyov, *Langmuir* **2018**, *34*, 3925.
[78] S. Shafeiei-Sabet, W. Y. Hamad, S. G. Hatzikiriakos, *Rheol. Acta* **2013**, *52*, 741.
[79] L. Lewis, M. Derakhshandeh, S. G. Hatzikiriakos, W. Y. Hamad, M. J. MacLachlan, *Biomacromolecules* **2016**, *17*, 2747.
[80] R. Nigmatullin, R. Harniman, V. Gabrielli, J. C. Muñoz-García, Y. Z. Khimyak, J. Angulo, S. J. Eichhorn, *ACS Appl. Mater. Interfaces* **2018**, *10*, 19318.
[81] J. Zhang, Q. Wu, M.-C. Li, K. Song, X. Sun, S.-Y. Lee, T. Lei, *ACS Sustain. Chem. Eng.* **2017**, *5*, 7439.
[82] K. Sahlin, L. Forsgren, T. Moberg, D. Bernin, M. Rigdahl, G. Westman, *Cellulose* **2018**, *25*, 331.
[83] D. Khandal, B. Riedl, J. R. Tavares, P. J. Carreau, M.-C. Heuzey, *Phys. Fluids* **2019**, *31*, 021207.
[84] S. Wang, K. Li, T. Xia, P. Lan, H. Xu, N. Lin, *Carbohydr. Polym.* **2022**, *276*, 118802.
[85] A. Koponen, J. Lauri, S. Haavisto, T. Fabritius, *Appl. Sci.* **2018**, *8*, 755.
[86] T. Saarinen, S. Haavisto, A. Sorvari, J. Salmela, J. Seppälä, *Cellulose* **2014**, *21*, 1261.
[87] E. Lasseuguette, D. Roux, Y. Nishiyama, *Cellulose* **2008**, *15*, 425.
[88] E. Saarikoski, T. Saarinen, J. Salmela, J. Seppälä, *Cellulose* **2012**, *19*, 647.
[89] A. Karppinen, T. Saarinen, J. Salmela, A. Laukkanen, M. Nuopponen, J. Seppälä, *Cellulose* **1807**, *2012*, 19.
[90] F. Martoïa, C. Perge, P. J. J. Dumont, L. Orgéas, M. A. Fardin, S. Manneville, M. N. Belgacem, *Soft Matter* **2015**, *11*, 4742.
[91] D. W. de Kort, S. J. Veen, H. Van As, D. Bonn, K. P. Velikov, J. P. M. van Duynhoven, *Soft Matter* **2016**, *12*, 4739.
[92] L. H. Switzer, D. J. Klingenberg, *Nord. Pulp Pap. Res. J.* **2003**, *18*, 141.
[93] R. Kerekes, C. J. Schell, *J. Pulp Paper Sci.* **1992**, *18*, J32.
[94] A. Celzard, V. Fierro, R. Kerekes, *Cellulose* **2009**, *16*, 983.
[95] H. W. Kropholler, W. W. Sampson, *J. Pulp Pap. Sci.* **2001**, *27*, 301.
[96] R. Wang, T. Rosen, C. Zhan, S. Chodankar, J. Chen, P. R. Sharma, S. K. Sharma, T. Liu, B. S. Hsiao, *Macromolecules* **2019**, *52*, 5499.
[97] T. Saito, T. Uematsu, S. Kimura, T. Enomae, A. Isogai, *Soft Matter* **2011**, *7*, 8804.
[98] R. Tanaka, T. Saito, T. Hänninen, Y. Ono, M. Hakalahti, T. Tammelin, A. Isogai, *Biomacromolecules* **2016**, *17*, 2104.
[99] M. J. Lundahl, M. Berta, M. Ago, M. Stading, O. J. Rojas, *Eur. Polym. J.* **2018**, *109*, 367.
[100] B. Wei, Q. Li, F. Jin, H. Li, C. Wang, *Energy Fuel* **2016**, *30*, 2882.
[101] L. Geng, N. Mittal, C. Zhan, F. Ansari, P. R. Sharma, X. Peng, B. S. Hsiao, L. D. Söderberg, *Macromolecules* **2018**, *51*, 1498.
[102] P. Rezayati Charani, M. Dehghani-Firouzabadi, E. Afra, A. Shakeri, *Cellulose* **2013**, *20*, 727.
[103] A. Naderi, T. Lindström, J. Sundström, *Cellulose* **2014**, *21*, 1561.
[104] X. Wang, J. Zeng, J. Y. Zhu, *Carbohydr. Polym.* **2022**, *295*, 119885.
[105] J. Liao, K. A. Pham, V. Breedveld, *Cellulose* **2021**, *28*, 813.
[106] H. Wang, J. J. Zhu, Q. Ma, U. P. Agarwal, R. Gleisner, R. Reiner, C. Baez, J. Y. Zhu, *Front. Bioeng. Biotechnol.* **2020**, *8*, 565084.
[107] C. Liu, H. Du, L. Dong, X. Wang, Y. Zhang, G. Yu, B. Li, X. Mu, H. Peng, H. Liu, *Ind. Eng. Chem. Res.* **2017**, *56*, 8264.
[108] R. Qu, Y. Wang, D. Li, L. Wang, *Food Hydrocoll.* **2021**, *121*, 106985.
[109] O. Nechyporchuk, M. N. Belgacem, F. Pignon, *Carbohydr. Polym.* **2014**, *112*, 432.
[110] F. Grüneberger, T. Künniger, T. Zimmermann, M. Arnold, *Cellulose* **2014**, *21*, 1313.
[111] I. H. Mondal, *Cellulose and Cellulose Derivatives: Synthesis*, Nova Science Publishers, Incorporated, Modification and Applications **2015**.
[112] R. L. Shogren, S. C. Peterson, K. O. Evans, J. A. Kenar, *Carbohydr. Polym.* **2011**, *86*, 1351.
[113] D. Lee, Y. Oh, J.-K. Yoo, J. W. Yi, M.-K. Um, T. Park, *Cellulose* **2020**, *27*, 9257.
[114] F. Bettaieb, O. Nechyporchuk, R. Khiari, M. F. Mhenni, A. Dufresne, M. N. Belgacem, *Carbohydr. Polym.* **2015**, *134*, 664.
[115] S. Shin, J. Hyun, *Carbohydr. Polym.* **2021**, *263*, 117976.
[116] H. Liimatainen, M. Visanko, J. A. Sirviö, O. E. O. Hormi, J. Niinimaki, *Biomacromolecules* **2012**, *13*, 1592.
[117] P. J. J. Dumont, S. Gupta, F. Martoïa, L. Orgéas, *Carbohydr. Polym.* **2023**, *299*, 120168.
[118] H. Haridevan, C. Chaleat, L. Pooley, D. A. C. Evans, P. J. Halley, D. J. Martin, P. K. Annamalai, *Polymer* **2022**, *255*, 125130.
[119] F. Montes, T. Fu, J. P. Youngblood, J. Weiss, *Constr. Build. Mater.* **2020**, *235*, 117497.

[120] Q. Ren, M. Wu, L. Wang, W. Zheng, Y. Hikima, T. Semba, M. Ohshima, *Carbohydr. Polym.* **2022**, *286*, 119320.
[121] Z. Zhou, Y. Yao, J. Zhang, L. Shen, H. Xu, J. Liu, B. Shentu, *Cellulose* **2022**, *29*, 8255.
[122] C. Liu, M.-C. Li, C. Mei, W. Xu, Q. Wu, *ACS Sustain. Chem. Eng.* **2020**, *8*, 10842.
[123] K. Jain, Z. Wang, L. D. Garma, E. Engel, G. C. Ciftci, C. Fager, P. A. Larsson, L. Wågberg, *Appl. Mater. Today* **2023**, *30*, 101703.
[124] S. Feng, Y. Yi, B. Chen, P. Deng, Z. Zhou, C. Lu, *ACS Appl. Mater. Interfaces* **2022**, *14*, 36060.
[125] G. Zhou, M. Li, C. Liu, Q. Wu, C. Mei, *Adv. Funct. Mater.* **2022**, *32*, 2109593.
[126] Z. J. Lee, S. Tong, T. Tang, Y. Lee, *J. Food Sci.* **2022**, *87*, 3542.
[127] H. Gao, B. Duan, A. Lu, H. Deng, Y. Du, X. Shi, L. Zhang, *Food Hydrocoll.* **2018**, *79*, 473.
[128] C. D. Armstrong, L. Yue, Y. Deng, H. J. Qi, *J. Food Eng.* **2022**, *330*, 111086.
[129] B. Wang, X. Zhao, C. Duan, J. Li, J. Zeng, J. Xu, W. Gao, K. Chen, *J. Colloid Interface Sci.* **2023**, *630*, 604.
[130] S. Guo, Y. Zhu, W. Xu, S. Huan, J. Li, T. Song, L. Bai, O. J. Rojas, *Carbohydr. Polym.* **2023**, *299*, 120154.
[131] C. Liu, M. Li, C. Mei, W. Chen, J. Han, Y. Yue, S. Ren, A. D. French, G. M. Aita, G. Eggleston, Q. Wu, *Ind. Crop. Prod.* **2020**, *150*, 112378.
[132] I. Larraza, J. Vadillo, T. Calvo-Correas, A. Tejado, L. Martin, A. Arbelaiz, A. Eceiza, *Polymer* **2022**, *14*, 4516.
[133] M. Pitton, A. Fiorati, S. Buscemi, L. Melone, S. Farè, N. Contessi Negrini, *Front. Bioeng. Biotechnol.* **2021**, *9*, 732689.
[134] K. Säljö, L. S. Orrhult, P. Apelgren, K. Markstedt, L. Kölby, P. Gatenholm, *Bioprinting* **2020**, *17*, e00065.
[135] M. Bordoni, E. Karabulut, V. Kuzmenko, V. Fantini, O. Pansarasa, C. Cereda, P. Gatenholm, *Cell* **2020**, *9*, 682.
[136] S. Im, G. Choe, J. M. Seok, S. J. Yeo, J. H. Lee, W. D. Kim, J. Y. Lee, S. A. Park, *Int. J. Biol. Macromol.* **2022**, *205*, 520.
[137] R. Olmos-Juste, B. Alonso-Lerma, R. Pérez-Jiménez, N. Gabilondo, A. Eceiza, *Carbohydr. Polym.* **2021**, *264*, 118026.
[138] D. Kam, A. Braner, A. Abouzglo, L. Larush, A. Chiappone, O. Shoseyov, S. Magdassi, *Langmuir* **2021**, *37*, 6451.
[139] P. Maturavongsadit, L. K. Narayanan, P. Chansoria, R. Shirwaiker, S. R. Benhabbour, *ACS Appl. Bio Mater.* **2021**, *4*, 2342.
[140] C. E. P. Silva, J. S. Bernardes, W. Loh, *Carbohydr. Polym.* **2023**, *302*, 120354.
[141] C. Liu, G. Zhou, Z. Li, M.-C. Li, X. Liu, M. S. Koo, Q. Wu, C. Mei, *Ind. Crop. Prod.* **2022**, *187*, 115402.
[142] Y. Wang, W. Xie, D. Wu, *Carbohydr. Polym.* **2020**, *231*, 115776.
[143] C. Liu, Z. Li, M.-C. Li, W. Chen, W. Xu, S. Hong, Q. Wu, C. Mei, *Carbohydr. Polym.* **2022**, *291*, 119573.
[144] D. Sonnleitner, S. Schrüfer, L. Berglund, D. W. Schubert, G. Lang, *J. Mater. Res.* **2021**, *36*, 3821.
[145] S. Cui, S. Zhang, S. Coseri, *Carbohydr. Polym.* **2023**, *300*, 120243.
[146] S. Moghadam, R. Karnati, H. E. Bode, J. S. Gill. Nanocrystalline cellulose and polymer-grafted nanocrystalline cellulose as rheology modifying agents for magnesium oxide and lime slurries. **2020**.
[147] F. Lessan, M. Karimi, J. L. Bañuelos, R. Foudazi, *Polymer* **2020**, *186*, 121969.
[148] Y. Jiang, J. Zhou, H. Shi, G. zhao, Q. Zhang, C. Feng, X. Xv, *J. Mater. Sci.* **2020**, *55*, 2618.
[149] J. A. Semba, A. Aron Mieloch, E. Tomaszewska, P. Cywoniuk, J. Dalibor Rybka, *Int. J. Bioprint.* **2023**, *9*, 621.

How to cite this article: A. K. Rana, V. K. Thakur, *J. Vinyl Addit. Technol.* **2023**, 1. https://doi.org/10.1002/vnl.22006